Antigen specificity shapes antibody functions in tuberculosis.

Joshua R. Miles[1#], Pei Lu[2#], Shuangyi Bai[3], Genesis P. Aguillón-Durán[4], Javier E. Rodríguez-Herrera[5], Bronwyn M. Gunn[3], Blanca I. Restrepo[4,6,7], and Lenette L. Lu[1,2,8]

[1]UT Southwestern Medical Center, Department of Immunology

[2]UT Southwestern Medical Center, Division of Infectious Diseases and Geographic Medicine, Department of Internal Medicine

[3]Paul G. Allen School of Global Health, College of Veterinary Medicine, Washington State University

[4]Department of Epidemiology, School of Public Health, University of Texas Health Science Center at Houston, Brownsville campus, Brownsville, TX, USA

[5]Departamento Estatal de Micobacteriosis, Secretaría de Salud de Tamaulipas, Reynosa 88630, Matamoros 87370, Tamaulipas, México

[6]School of Medicine, South Texas Diabetes and Obesity Institute, University of Texas Rio Grande Valley, Edinburg, TX, USA

[7]I.CARE and Population Health, Texas Biomedical Research Institute, San Antonio, TX, USA

[8]Parkland Health

[#]equal contribution

Abstract

Tuberculosis (TB) is the number one infectious disease cause of death worldwide in part due to an incomplete understanding of immunity. Emerging data highlight antibody functions as correlates of protection and disease across human TB. However, little is known about how antibody functions impact *Mycobacterium tuberculosis (Mtb)*, the causative agent. Here, we use antigen specificity to understand how antibodies mediate host-*Mtb* interactions. We focus on *Mtb* cell wall and ESAT-6 & CFP-10, critical bacterial structural and secreted virulence proteins. In polyclonal IgG from TB patients, we observe that antigen specificity alters IgG subclass and glycosylation that drives Fc receptor binding and effector functions. Through in vitro models of *Mtb* macrophage infection we find that *Mtb* cell wall IgG3, sialic acid, and fucose increase opsonophagocytosis of extracellular *Mtb* and bacterial burden, suggesting that some polyclonal IgG enhance disease. In contrast, ESAT-6 & CFP-10 IgG1 inhibits intracellular *Mtb*, suggesting that antibodies targeting secreted virulence factors are protective. We test this hypothesis by generating a mAb that reacts to ESAT-6 & CFP-10 and show that it alone inhibits intracellular *Mtb*. Understanding which antigens elicit antibody mediated disease enhancement and or protection will be critical in appreciating the many roles for antibodies in TB.

Introduction

Antibodies are leveraged in vaccines, diagnostics, and therapeutics in many infectious diseases but for tuberculosis (TB), their role is unclear (1-5). Unlike other pathogens, the presence of antibodies reactive to *Mycobacterium tuberculosis* (*Mtb*), the causative agent, is linked to neither protection nor disease (6-9). In contrast, cellular immunity has been thought to be the cornerstone of protection with loss of function in humans and animal models associated with decreased survival after *Mtb* challenge (10). However, enhanced T cell responses through immunomodulation such as programmed cell death protein 1 inhibitors paradoxically worsen disease (11, 12). Moreover, the first large phase IIB clinical trial of a TB vaccine designed to boost Th1 and Th17 responses, MVA85A, showed no protection (13), and unexpectedly, CD4 T cell responses associated with increased whereas Ag85A IgG titers linked to decreased risk of disease. In revisiting the paradigm of protection in TB (3), a significant gap in knowledge is the role of antibodies.

Antibodies function by the combination of the Fab domain binding to the antigen and Fc domain engaging receptors on immune cells to induce effector functions (2, 5). Diversity within the Fc domain in subclass and post-translational glycosylation regulate binding to activating and inhibitory Fc receptors (FcRs) that initiate downstream signaling and immune cell activation (14-17). In mice, loss of activating FcR signaling decreases survival after *Mtb* challenge (18). Conversely, loss of inhibitory FcR signaling limits bacterial burden. In humans, the activating FcγRIIIa is associated with protection in latent TB as compared to disease in active TB (19). We have shown that IgG Fc properties and effector functions diverge in latent and active TB (20, 21). Moreover, in an in vitro macrophage model of *Mtb* infection, treatment with IgG from latent compared to active TB leads to decreased *Mtb* burden and increased antimicrobial activities (20). These findings suggest that antibodies from TB patients are protective, disease enhancing, or both. Here, we focus on *Mtb* antigen specificity to understand how antibody functions impact *Mtb* and begin to define mechanisms of protection and disease.

With over 4000 open reading frames, glycans, and glycolipids, the immunodominant *Mtb* repertoire in humoral immunity is not known (22). As such, a mixture of proteins from bacterial culture (purified protein derivative (PPD)) has been used in many studies to identify reactivity to *Mtb* (6, 23, 24). However, the Fab domain impacts Fc functions such that changing the Fab domain to recognize different epitopes while maintaining the Fc domain alters the ability of the antibody to bind to FcRs and initiate effector functions. Functionally, changing the Fab domain sufficiently alters Fc domain mediated protection in animal infection models of influenza and Cryptococcus (25-27). To this point, mAbs that target different *Mtb* surface and cell wall antigens (LAM, PstS1, and heparin-binding hemagglutinin are examples) utilize different FcRs to impact *Mtb* (28-31). Beyond testing mAbs in isolation, understanding how antigen specificity impacts polyclonal antibody Fc functions highlights potential mechanisms of infection and disease in humoral immune responses where antibodies function collectively.

In this study, we leverage the heterogeneity of polyclonal IgG responses in human latent and active TB to understand the impact of antigen specificity on subclass, post-translational glycosylation and Fc effector functions. For each individual TB patient, we measure the impact of their IgG on infection using macrophage models that examine *Mtb* in its extracellular and intracellular states of the life cycle. By linking IgG Fc properties to *Mtb* burden we discover that with opsonophagocytosis of extracellular *Mtb*, *Mtb* cell wall IgG enhances disease through IgG3, sialic acid, and fucose directed Fc receptor binding. In comparison, with antibody treatment of macrophages after *Mtb* infection where the population is intracellular, we find that IgG reactive to ESAT-6 & CFP-10 negatively correlates with bacterial burden, suggesting antibodies that recognize secreted *Mtb* virulence factors are protective. We test this hypothesis by generating a monoclonal human IgG1 that recognizes ESAT-6 and CFP-10 and show that it alone is sufficient to inhibit intracellular *Mtb*. These data show that in latent and active TB, antigen specificity influences how IgG impacts *Mtb* and helps define mechanisms of antibody mediated disease enhancement and protection.

Results

Antigen specificity alters the capacity to differentiate latent and active TB by IgG subclass.

We began with the framework of latent TB infection and active TB disease to understand the impact of antigen specificity on antibody functions in the context of protection and disease as reflected by the clinical TB spectrum (Table). Individuals with latent TB infection have decreased risk of progression to active TB disease compared to the uninfected (32). Latent TB infection was diagnosed by the presence of a blood T cell-IFNγ response to *Mtb* ESAT-6, CFP-10, and TB7.7, absence of signs and symptoms of disease, and history of exposure to TB. Active TB was defined by the presence of clinical disease and detectable *Mtb* (33-35). Individuals from the same area with no history of or exposure to TB were used as endemic controls to account for environmental non-tuberculous mycobacteria and other geographical variations that impact the development of immunity (36-40).

To systematically approach the >4000 *Mtb* protein antigens (41), we balanced breadth and specificity with individual and fractions of mixed antigen preparations from bacteria in culture. Since the dominant repertoire of epitopes recognized by antibodies in TB is unclear (22), many studies use purified protein derivative (PPD) that reflects the bacterial cytosol and cell wall though it can be skewed towards a subset of antigens (6, 23, 24). In addition to PPD, we used protein fractions enriched in components of *Mtb* cell wall, cytosol, and secretions into the culture (culture filtrate) (42-44) on the premise that localization with respect to the bacteria could impact the sensing, processing, and development of antibodies (29, 30, 45-48). In addition to protein mixes, we chose the well-studied secreted bacterial virulence factor complexes Ag85A & Ag85B (49) and ESAT-6 & CFP-10 (50). As a non-*Mtb* control from a common pulmonary pathogen with high seroprevalence in adults, we used a mixture of proteins from respiratory syncytial virus (RSV) (51). Together these antigens enabled the evaluation of

humoral immunity targeting bacterial structural, metabolic, and immune modulatory functions important for survival in the host.

We found that antigen specificity changes how IgG titers relate to disease, consistent with the variable experience using *Mtb* reactive IgG for serological diagnoses (52, 53). Only *Mtb* cell wall IgG significantly distinguished active from latent TB (Figure 1A) with differences in levels of IgG1 and IgG2, not IgG3 and IgG4 (Figure 1B). In contrast, IgG reactive to PPD, *Mtb* cytosolic proteins, culture filtrate, and the virulence factors Ag85A & Ag85B and ESAT-6 & CFP-10 could not distinguish between clinical TB states (Figure 1A and 1C) like control RSV (Supplemental Figure 1). To further examine the impacts of antigen specificities, we focused on *Mtb* cell wall as the only antigen specific IgG that predicts disease and ESAT-6 & CFP-10 as the most similar between latent and active TB.

Antigen specificity separates antibody Fc domain glycosylation in latent and active TB.

Antibodies function through the combinatorial diversity of the Fab domain via its antigenic repertoire and the Fc domain with subclass distribution and post-translational N-glycosylation (2, 14-17). On a single conserved asparagine residue on the IgG Fc domain (N297) is a core biantennary complex of mannose and N-acetylglucosamine (GlcNAc) (Supplemental Figure 2A). Addition and subtraction of galactose, sialic acid, bisecting GlcNAc, and fucose to the core structure generates heterogenous individual glycan structures. For every single individual cohort sample, we measured glycosylation patterns on IgG reactive to ESAT-6 & CFP-10, *Mtb* cell wall, control RSV, and total bulk IgG Fc domains (Figure 2A, Supplemental Figure 2B). We summarized the individual glycans into total sialic acid (S), galactose (G), fucose (F), bisecting GlcNAc (B), fucose with sialic acid (F w/ S), and fucose without sialic acid (F w/o S) (Figure 2B, Supplemental Figure 2C and 2D). We observed that antigen specific compared to total bulk IgG had higher sialic acid, galactose, and bisecting GlcNAc (Figure 2B and Supplemental Figure 2D). Within antigen specific IgG, *Mtb* antigens distinguished

themselves from RSV through even higher sialic acid, galactose, and bisecting GlcNAc but lower fucose (Figure 2B and Supplemental Figure 2D). Within *Mtb*-reactive IgG, bisecting GlcNAc was not different. Rather, *Mtb* cell wall compared to ESAT-6 & CFP-10 IgG had lower sialic acid and galactose and higher fucose, with the major changes occurring in fucose without sialic acid. Thus, each antigen specificity appeared to have a unique glycosylation pattern, consistent with B cell intrinsic rather than extrinsic mechanisms dominating IgG glycosylation (54, 55). Moreover, like subclass distribution, Fc glycosylation changes with antigen specificity in TB.

Because we previously reported that differential IgG glycosylation was linked to latent and active TB (20, 21, 56-58), we evaluated how clinical state in addition to antigen specificity impacted IgG glycosylation in this cohort. Using principal components analysis and hierarchical clustering to globally assess the individual glycoform patterns across all patients, we confirmed prior findings that IgG Fc glycosylation was separated out by latent and active TB (Figure 2C). However, we found that antigen specificity made a greater impact (Figure 2D and Supplemental Figure 2F). Thus, post-translational glycosylation is influenced by antigen specificity more than clinical TB state.

Antibody Fc effector functions diverge more by antigen specificity than latent and active TB.

The differences in subclass distribution and Fc N-glycosylation suggested that *Mtb* cell wall compared to ESAT-6 & CFP-10 IgG diverge in their abilities to bind to Fc receptors (FcRs) and initiate immune cell effector functions. To evaluate the impact of antigen specificity on FcR engagement, we measured binding to high and low affinity FcRs that have been described to impact TB: FcγRI (28, 59, 60), FcγRIIa (28, 29, 46), FcγRIIb (18, 28, 29, 46), FcγRIIIa (19, 20, 29), and FcRn (30, 61) (Supplemental Figure 3A). Because Fc functions involve steps beyond FcR binding including adaptor-mediated signaling and feedback we further evaluated with the cell-based assays antibody dependent natural killer cell activation (ADNKA) that induces cellular

cytotoxicity and antibody dependent cellular phagocytosis (ADCP) (Supplemental Figure 3B and C). Both have been linked to protection and disease in human TB (19, 20, 28, 56). Through principal components analysis we found that Fc functions separated by antigen specificity more than TB status (Figure 3A and 3B). ADNKA markers characterized ESAT-6 & CFP-10 while ADCP highlighted *Mtb* cell wall IgG functions. Binding to individual FcRs minimally distinguished the antigens. These data demonstrate that measurements of IgG engagement of multiple FcRs to induce cell signaling and activation capture more distinctions between *Mtb* antigens as compared to simply binding to individual FcRs. While previous work ((20)) showed Fc receptor binding and effector function differences between latent and active TB IgG, these data show that antigen specificity more than clinical TB states influence IgG Fc effector functions. Moreover, differences in IgG subclass, glycosylation that drive Fc effector functions suggested that antigen specificity alters how antibodies could modulate *Mtb*.

Latent and active TB IgG differentially impact Mtb in macrophage infection.

To begin to evaluate the impact of antigen specific antibodies on *Mtb*, we used in vitro models of macrophage infection. Monoclonal and polyclonal antibodies have been shown to mediate differential uptake of extracellular *Mtb* into the macrophage (28, 29, 62-64). This quintessential immune cell niche has the capacity to restrict and also permit bacterial replication (20, 28, 29, 58, 62, 63, 65-68). We evaluated how polyclonal IgG from this cohort impacts *Mtb* burden resulting from opsonophagocytosis of extracellular bacteria into the macrophage. We used a virulent *Mtb* H37Rv reporter strain (*Mtb*-276) where luminescence correlates with bacterial burden (Supplemental Figure 4A) (69, 70) in primary human monocyte derived macrophages (pMDM) that express FcRs involved in TB (FcγRI, FcγRIIa, FcγRIIb, FcγRIIIa, and FcRn). We incubated bacteria with IgG from each individual patient and used the opsonized *Mtb* to infect pMDMs at an MOI=1 (Figure 4A). We used a low MOI to mimic the high infectivity and paucibacillary nature of *Mtb* and limit the macrophage toxic effects of non-physiological high

loads of bacteria and their components. We quantified *Mtb* growth after infection (Supplemental Figure 4B) and found that *Mtb* burden was lower when opsonized by IgG from individuals with latent compared to active TB (Figure 4B). These data demonstrated that polyclonal IgG from individuals across the spectrum of protected latent and diseased active TB have properties that alter uptake of extracellular *Mtb* into the macrophage and its subsequent growth.

While extracellular bacteria are present during initial infection and likely active TB particularly with advanced disease, the majority of *Mtb* is thought to be intracellular (65, 66, 71, 72). We have previously shown that intracellular *Mtb* is differentially impacted by polyclonal IgG pooled from latent and active TB patients (20). Here, we enhanced the resolution of these prior experiments by evaluating the impact of IgG from each individual latent and active TB patient on intracellular bacteria. We infected macrophages first, washed away the extracellular *Mtb*, then treated the *Mtb* infected macrophages with IgG (Figure 4C). Consistent with prior studies using IgG pooled from latent and active TB patients, on the level of individual TB patients intracellular *Mtb* burden was lower after treatment with IgG from latent compared to active TB (Figure 4D). Thus, polyclonal IgG from individuals across latent and active TB have properties that impact intracellular *Mtb* replication after infection has occurred. The results of these extracellular (Figure 4B) and intracellular (Figure 4D) assays were then leveraged to understand the relationship of antigen specificity on modulation of *Mtb* during macrophage infection by IgG in latent and active TB.

Mtb cell wall IgG enhances Mtb burden in opsonophagocytosis of extracellular bacteria.

To assess the impact of antigen specificity on opsonophagocytosis of *Mtb*, we evaluated the relationships between antigen specific IgG properties and *Mtb* burden after extracellular bacteria is opsonized, taken up, and then replicates in the macrophage. We used simple linear regression to test the dependence of *Mtb* burden on *Mtb* cell wall specific subclass, FcR binding, and Fc effector functions. We found that the *Mtb* burden from opsonophagocytosis and

subsequent growth in the macrophage was dependent on *Mtb* cell wall IgG3 and binding to high (FcRn and FcγRI) and low (FcγRIIa and FcγRIIb) affinity FcRs (Figure 5A) contrasting control RSV (Supplemental Figure 5). There were no relationships in the context of intracellular bacteria with antibody treatment after macrophage infection (Figure 5B). To incorporate the combination of subclass levels and glycosylation, we next used multiple linear regression. We found that extracellular and not intracellular *Mtb* burden was enhanced by both fucose and sialic acid (Figure 5C and 5D), the glycans that most significantly distinguished *Mtb* cell wall from ESAT-6 & CFP-10 IgG (Figure 2B). As has been reported by others (28), these relationships occurred only in latent and not active TB disease and linked to higher potency of IgG Fc functions (Supplemental Figure 6). These data show that with high Fc potency in latent compared to active TB, *Mtb* cell wall IgG functions through opsonizing extracellular *Mtb* prior to and not after infection.

ESAT-6 & CFP-10 IgG inhibits intracellular Mtb.

In contrast to *Mtb* cell wall, ESAT-6 & CFP-10 IgG appeared to inhibit *Mtb* after infection and had no impact on opsonophagocytosis of extracellular bacteria prior to infection (Figure 6A and 6B). More specifically, ESAT-6 & CFP-10 IgG1 negatively linked to intracellular bacterial burden and growth rate (Figure 6C and 6D). This was also observed in latent and not active TB though not linked to changes in Fc functional potency (Supplemental Figure 6). These data suggested that some ESAT-6 & CFP-10 IgG in latent TB have the capacity to protect.

To test the ability of ESAT-6 & CFP-10 IgG1 to inhibit *Mtb*, we cloned a monoclonal human IgG1 (ESAT-6 mAb) that recognizes ESAT-6, CFP-10, and the combination (Supplemental Figure 8A-C). Treatment of *Mtb* infected macrophages with the ESAT-6 mAb as compared to isotype control led to decreased intracellular *Mtb* burden in a dose-dependent manner (Figure 6E and 6F and Supplemental Figure 8D and 8E). These data show that in latent TB, IgG recognizing the secreted *Mtb* virulence factors ESAT-6 & CFP-10 function by targeting

intracellular bacteria after infection has been established in the macrophage and not opsonization of extracellular *Mtb*.

Discussion

Building from studies in latent and active TB showing that antibody functions correlate with protection and disease, here we use *Mtb* cell wall proteins and the secreted virulence complex ESAT-6 & CFP-10 to begin to unravel the underlying mechanisms. We show that antigen specificity alters IgG subclass distribution, glycosylation, and Fc effector functions to reveal divergence in how disease and protection are mediated and the bacterial population targeted. When *Mtb* cell wall IgG in latent TB is used to opsonize extracellular bacteria before macrophage infection, *Mtb* burden is enhanced (Figure 5A). This is through IgG3, the subclass with the highest ability to induce Fc receptor binding and effector functions (73). This is consistent with links to FcγRI, FcγRIIa, and FcγRIIb that drive antibody dependent cellular phagocytosis, as well as the high affinity FcRn (Figure 5A). In addition, the presence of Fc sialylation and absence of Fc fucosylation link to *Mtb* burden (Figure 5C), indicating that glycan modulation of Fc receptor binding described in the literature is also important (17, 74-77). In contrast, ESAT-6 & CFP-10 IgG1 in latent TB targets the intracellular *Mtb* population that is established after infection (Figure 6B). Its protective capacity is shown in both polyclonal and mAb studies where ESAT-6 & CFP-10 IgG1 alone is sufficient to measurably inhibit bacterial burden (Figure 6E and 6F). Thus, *Mtb* antigens do not all elicit the same Fc effector function. Rather, diverse Fc properties and functions link to different antigens, and in combination with the nature of the bacterial target determine how antibodies modulate *Mtb* infection.

Matching age and sex in the clinical groups of latent and active TB, stringent diagnostic and exclusion criteria that limit confounding factors, and the use of endemic negatives strengthens this study. However, latent and active TB represent a portion of the human TB spectrum (4, 78). Evaluating individuals highly exposed but not considered to have classical

latent TB (58), during and after antimicrobial treatment (56, 79, 80), with reinfection (81), and comparing those with and without BCG vaccination (82, 83) along with clinical outcomes (57) would orthogonally validate our findings. Additionally, these data reflect a fraction of the *Mtb* antigen repertoire (22, 41). Using this approach systematically would identify additional bacterial antigens that elicit polyclonal antibody responses impacting *Mtb* throughout its life cycle in the host.

One possible way that different antigens from the same bacteria could elicit such divergent antibody Fc properties could be immune priming. *Mtb* cell wall proteins cross-react with environmental NTMs (36-40, 45). The prevalence of ESAT-6 & CFP-10-like proteins is comparatively far less such that it is used for current T-cell based diagnostics (35). As such, the antibodies that react to *Mtb* cell wall could result from a priming effect due to pre-existing NTM immunity. In contrast, antibodies reactive to ESAT-6 & CFP-10 could represent responses to de novo exposure (37). Further studies that assess the effect of pre-existing immunity to NTMs on antigen avidity and Fc properties after *Mtb* infection would help evaluate this possibility (36).

Antibodies targeting *Mtb* cell wall antigens have been described to enhance and inhibit *Mtb*. Monoclonal IgG1 targeting the bacterial surface exposed heparin binding hemagglutinin (HBHA), show that enhancement of entry into epithelial cells is possible through FcRn (30). Monoclonal IgG targeting *Mtb* cell wall proteins (PstS1, HspX, and LpqH) (29, 84, 85) and monoclonal and polyclonal IgG targeting the bacterial glycan arabinomannan inhibit *Mtb* through Fc dependent and independent mechanisms (28, 62-64). Thus, while the overall mixture of *Mtb* cell wall proteins enhances disease in this study, it is likely that within the cell wall fraction, some antigens induce protective and others disease enhancing antibodies.

Antibody dependent enhancement of infection has been described in viral and bacterial infections (86-89) including the intracellular pathogens Legionella (90) and Leishmania (91, 92) in macrophages that involve cross-reactive and Fc receptor mediated mechanisms. Because the macrophage is also an important niche for *Mtb* where the bacteria grows and dies, antibody

dependent enhancement of infection has been hypothesized to occur. These data show that macrophage FcRs can be engaged by *Mtb* cell wall and not ESAT-6 & CFP-10 polyclonal IgG to enhance disease.

IgG targeting the secreted virulence factors ESAT-6 & CFP-10 inhibit intracellular bacteria, conferring protection after *Mtb* has established infection (Figure 6B – 6F). Comparative genomics show that strains are attenuated with the absence of ESAT-6 & CFP-10, and then virulence is re-established with the introduction of ESAT-6 & CFP-10 (93, 94). Moreover, an anti-ESAT-6 nanobody blocks intracellular *Mtb* replication (95). Because the large size of intact human IgG compared to a nanobody limits cellular penetration, direct neutralization may not be the sole mechanism of IgG1 mediated bacterial inhibition. A complementary scenario is that ESAT-6 & CFP-10 secreted away from *Mtb* (50, 96, 97) enables immune complex formation separate from the bacteria to engage Fc receptors and induce macrophage effector functions. Our data show that the ability to activate NK cells through FcγRIIIa and induce cellular cytotoxicity highlights ESAT-6 & CFP-10 IgG (Figure 3). A similar process could be occurring with macrophages who also carry out cellular cytotoxicity. Monoclonal Fc modifications to enhance and inhibit cellular cytotoxicity could further evaluate mechanisms (98).

Notably, antibody mediated disease enhancement and protection for *Mtb* were observed in the context of latent and not active TB (Figure 5 and 6). This difference with respect to TB status has been reported with arabinomannan specific IgG (28) and thought to be due to higher functional potency. In this study, increased Fc effector functional potency may explain the observations with *Mtb* cell wall, not ESAT-6 & CFP-10 IgG (Supplemental Figure 6). As such there are two additional possibilities to consider. First, high levels of IgG in active TB may interfere with antibody functions in a prozone-like effect (99-101). Second, the large spectrum of infection identified by the clinical diagnosis of latent TB enables the ability to capture differences in antibody functions that active TB in this cohort does not. Latent TB describes individuals with infection that has been progressing and regressing for years if not decades (57, 78, 102, 103).

Active TB in these studies represent only those within 7 days of diagnosis and in the absence of treatment. Longitudinal studies that follow clinical outcomes of latent TB as well as extending the spectrum beyond active TB to follow treatment would help clarify the findings for *Mtb* cell wall and ESAT-6 & CFP-10 IgG made here.

What *Mtb* antigens are relevant for humoral immunity is unclear but essential to understand if we are to harness antibodies for TB diagnostics, vaccines, and therapeutics. Through conventional approaches that define what is relevant by antigen specific antibody titers (104, 105), *Mtb* cell wall IgG would be considered a correlate of disease and ESAT-6 & CFP-10 IgG would be less interesting due to its lack of association with a specific clinical state. Through our antibody functional data that evaluate *Mtb* in its extracellular and intracellular stages in the host (65, 66, 71, 72), *Mtb* cell wall IgG would be considered pathogenic and ESAT-6 & CFP-10 IgG protective. That pathogenic and protective IgG simultaneously exist could explain why some passive serum transfer experiments show inhibition while others enhancement of bacterial burden, contributing to the lack of clarity in the role of humoral immunity in TB (6-9). This study represents a starting point with IgG from blood. Extending evaluations to IgA and IgM in pulmonary and peripheral responses will highlight isotype and compartment specific distinctions in mucosal (36, 84, 106-109) and systemic immunity critical to understanding how antibodies impact TB.

Materials and Methods

Sex as a biological variable

To address sex as a biological variable, the experimental groups were matched by sex and statistical analyses were performed to account for sex.

Study design

Adults were recruited from the Texas/Mexico border (2006-2010) (33). Latent TB (n=18) was defined by a positive interferon γ release assay (IGRA) TSPOT or QuantiFERON with no history of prior TB diagnosis or treatment, and no clinical signs and symptoms of active TB disease. Active TB (n=19) was defined by sputum acid fast bacilli smear and culture in combination with clinical signs and symptoms of disease. Endemic controls (n=8) were defined by negative TSPOT or QuantiFERON with no history, clinical signs and symptoms, or exposure to TB. To limit confounding variables, groups for latent and active TB were matched by age and sex (57, 110), tested negative for HIV and type 2 diabetes as defined by WHO criteria (81, 111-116), and received <8 days TB treatment (56, 79). Written informed consent was obtained from study participants and approved by institutional IRBs.

Sample Collection

Blood samples were collected by venipuncture in sodium heparin tubes, plasma isolated by centrifugation, aliquoted, stored at −80°C, and heat-inactivated (30 min, 55C) prior to use.

IgG purification

Polyclonal IgG from patient samples was isolated by negative selection via Melon Gel resin (Thermo Fisher), concentrated by ultra-centrifugal filtration (Millipore Sigma), and quantified by ELISA (Mabtech) per manufacturers' instructions.

Monoclonal hIgG1 plasmid design and construction

An anti-ESAT-6 VH/k sequence (GenBank: LC189555.1 (117)) was synthesized and cloned into a pUC19 vector with a human IgG1 Fc domain as previously described in detail (98). Donor and destination plasmids were combined in a single digestion-ligation reaction to generate an expression plasmid encoding the heavy and light chains with BsaI-HF (NEB) and

374 T4 ligase (NEB), transformed into Stellar competent cells (Clontech) and selected by
375 kanamycin.
376
377 *Production of monoclonal hIgG1*
378 As previously described (98), plasmids were transfected into 293F suspension cells
379 using Polyethylenimine (PEI) (Polysciences). Supernatants were collected 5 days after
380 transfection and IgG was isolated by protein G magnetic beads (16 hours, 4C), eluted using
381 Pierce IgG Elution Buffer (Thermo Fisher), and neutralized with Tris-HCl pH 8.0.
382
383 *Cell lines*
384 NK92 cells expressing human FcγRIIIa (CD16.NK-92) (ATCC) were maintained in α-
385 MEM without nucleosides (Thermo Fisher), 2mM L-glutamine (Thermo Fisher), 1.5g/L sodium
386 bicarbonate (Thermo Fisher), 0.02mM folic acid (Alfa Aesar), 0.2mM inositol (MP Biomedicals),
387 0.1mM β-mercaptoethanol (Thermo Fisher), 100U/mL IL-2 (STEMCELL Technologies), 12.5%
388 horse serum (Cytiva), and 12.5% FBS (Gibco), 37C, 5% CO_2. THP-1 cells (ATCC) were
389 cultured in RPMI-1640 (Sigma-Aldrich), 10% FBS, 2mM L-glutamine, and 10mM HEPES
390 (Thermo Fisher), and 55μM beta-mercaptoethanol, 37C, 5% CO_2. Freestyle 293F cells (Thermo
391 Fisher) were maintained in a shaking incubator at 125 RPM, 37C, 8% CO_2 in Freestyle 293F
392 expression medium (Thermo Fisher).
393
394 *Primary human monocyte derived macrophages*
395 Monocytes were isolated from buffy coats obtained from healthy HIV negative adults by
396 CD14 positive selection (Miltenyi) per manufacturer's instructions and matured by adhesion for
397 7 days in RPMI-1640, 10% FBS, 2mM L-glutamine, and 10mM HEPES.
398
399 *Mycobacterium tuberculosis H37Rv*

A virulent H37Rv (*Mtb*-276) strain expressing luciferase under the P_{hsp60} promotor was cultured using Middlebrook 7H9 (BD) with 0.05% Tween-80 (Millipore Sigma) and Zeocin (20µg/mL) (Invivogen) to log-phase at 37C (69, 70), washed with PBS, and passed through a 5µm filter (Millipore Sigma) to obtain a single cell suspension prior to infection (MOI=1). Enumeration by colony forming units was performed using serial dilutions on 7H10 medium (BD).

Antigens

H37Rv purified protein derivative (PPD) (Statens Serum Institute), culture filtrate (BEI), cytosolic proteins (BEI), and cell wall fractions (BEI), as well as ESAT-6 (BEI), CFP-10 (BEI), Ag85A (BEI), Ag85B (BEI) were used as *Mtb* antigens. As controls, respiratory syncytial virus G (BEI) and F (BEI) proteins were used.

Quantification of antigen specific IgG and subclasses

Customized Luminex assays were used to measure antigen specific IgG and subclass levels as previously described (76, 118, 119). Carboxylated microspheres (Bio-Rad, MC100 series) were coupled to protein antigens using an NHS-ester reaction (Thermo Fisher, cat#A32269) following manufacturer's instructions. Serial dilutions of IgG purified from each individual patient sample (0.18, 0.06, 0.02 ug/mL) was added to antigen-coupled beads (18hours, 4C) and washed. PE-conjugated antibodies detecting total IgG (JDC-10, Southern Biotech), IgG1 (4E3, Southern Biotech), IgG2 (HP6002, Southern Biotech), IgG3 (HP60502, Southern Biotech), and IgG4 (HP6025, Southern Biotech), were added (2 hours, room temperature), washed with PBS 0.05% Tween-20, and re-suspended in PBS to acquire fluorescence intensity on Magpix (Luminex). The relative level of antigen specific antibodies was defined as the area under the curve (AUC) calculated from the serial dilutions for each individual sample.

Quantification of antigen binding with ESAT-6 mAb

Customized Luminex assays were used to measure antigen binding (76, 118, 119). Antigens were coupled to carboxylated microspheres as described above. Serial dilutions of monoclonal hIgG1 (15, 1.5, 0.15 µg/mL) were added to antigen-coupled beads. PE-conjugated anti-human IgG1 was used for detection and fluorescence intensity acquired on Magpix (Luminex) as described above.

Isolation of antigen specific and total IgG Fc domains

Antigens were biotinylated using EZ-Link Sulfo-NHS-LC-Biotin (Thermo Fisher) per manufacturer's instructions and coupled to streptavidin beads (NEB). Patient plasma (diluted 1:5 in 0.5M NaCl, 20mM Tris-HCl, 1mM EDTA, pH 7.5) was added to antigen-coupled beads for immunoprecipitation of ESAT-6 & CFP-10 (18 hours, 4C), *Mtb* cell wall (2.5 hours, room temperature), and RSV (18 hours, 4C) specific antibodies. For bulk total IgG, protein G beads (Millipore Sigma) were used (2 hours, room temperature). IdeZ (NEB) (1.5 hours, 37C) was used to cleave the Fc domain for subsequent glycan isolation.

N-linked glycan isolation and quantification

Isolation, labeling, and quantification of N-linked glycosylation are previously described (76, 119-121). In brief, isolated Fc domains were denatured (10 minutes, 95C) prior to enzymatic glycan release with PNGaseF (NEB) per manufacturer's instructions (18 hours, 37C). For antigen specific IgG Fc domains, released glycans were isolated with Agencourt CleanSEQ beads (Beckman Coulter). For total bulk IgG Fc domains, proteins were precipitated in ice-cold ethanol. Glycan-containing supernatants were dried using a CentriVap, then labeled with 8-aminoinopyrene-13,6-trisulfonic acid (APTS) (Thermo Fisher) in 1.2M citric acid and 1M $NaBH_3CN$ in tetrahydrofuran (Thermo Fisher), and 0.5% NP-40 (NEB) (3 hours, 55C). Excess

APTS was removed using Bio-Gel P-2 size exclusion resin (Bio-Rad) (antigen specific glycans) and Agencourt CleanSEQ beads (total bulk glycans). Labeled samples were run with a LIZ 600 DNA ladder (Thermo Fisher) in Hi-Di formamide (Thermo Fisher) on an ABI Gene Analyzer 3500XL and analyzed using GlycanAssure version 1.0 (Thermo Fisher).

Measurement of antigen specific IgG Fc receptor binding

Customized Luminex assay was used to measure antigen specific IgG FcR binding as previously reported (76, 118, 119, 122). As described above, carboxylated microspheres were coupled to protein antigens using an NHS-ester reaction and serial dilutions of IgG purified from each individual patient sample (0.18, 0.06, 0.02 ug/mL) was added to antigen-coupled beads. Recombinant FcRs (FcγRIIIa, FcγRIIa, FcγRIIb, and FcRn) (R&D Systems) were conjugated with phycoerythrin (PE) (Abcam) per manufacturer's instructions. PE-conjugated FcγRIIIa, FcγRIIa, and FcγRIIb were added at pH 7.4; PE-conjugated FcRn at pH 6.0 (123) (2 hours, room temperature). FcγRI recombinant protein (R&D Systems) was added to IgG coated beads and then incubated with mouse anti-human FcγRI (10.1, Santa Cruz) (1 hour, room temperature) followed by PE-conjugated goat anti-mouse (Southern Biotech) (1 hour, room temperature) for detection. Fluorescence intensity was acquired on a Magpix instrument (Luminex), and AUC calculated as described above.

Antibody dependent cellular phagocytosis

The THP-1 phagocytosis assay of antigen-coated beads is previously described (76, 119, 124). *Mtb* cell wall, ESAT-6 & CFP-10, or RSV antigen mix were biotinylated with EZ-Link Sulfo-NHS-LC-Biotin following manufacturer's instructions and coupled to FluoSpheres NeutrAvidin beads (Molecular Probes) (16 hours, 4C). Antigen-coupled beads were incubated with 100µg/mL polyclonal IgG purified from each patient and then added to THP-1 cells (1x10^5 per well) (37°C, 16 hours). After fixation with 4% PFA, bead uptake was measured by flow

cytometry on a BD-LSR Fortessa and analyzed by FlowJo v10. Phagocytic scores were calculated as the integrated median fluorescence intensity (MFI) (% bead-positive frequency × MFI/10,000) (125).

Antibody dependent natural killer cell activation

Antibody dependent NK cell activation is previously described (76, 119, 126). ELISA plates were coated with antigen (300ng/well) (18 hours, 4C), washed 3 times with PBS, blocked with 5% BSA (18 hours, 4C), and then washed 3 times. Purified polyclonal IgG from each patient (100µg/mL) was added (2 hours, 37C), followed by CD16a.NK-92 cells (5×10^4 cells/well) with brefeldin A (Biolegend), Golgi Stop (BD Biosciences) and anti-CD107a (H4A3, Biolegend) (5 hours, 37C). Cells were stained with anti-CD56 (5.1H11, Biolegend) and anti-CD16 (3G8, Biolegend) and fixed with 4% PFA. Intracellular cytokine staining to detect IFNγ (B27, Biolegend) and TNFα (Mab11, BD Biosciences) was performed in permeabilization buffer (Biolegend). Markers were measured using a BD LSR Fortessa and analyzed by FlowJo as described above.

Macrophage Mtb infections

To test the impact of antibodies on the uptake of extracellular *Mtb* into the macrophage and its subsequent replication, purified IgG from each individual patient was incubated with log-phase *Mtb* (4 hours, 37C). The IgG (100ug/mL) opsonized *Mtb* were used to infect primary human monocyte derived macrophages (5x10^4 cells/well) at an MOI=1.

To test the impact of antibodies on intracellular *Mtb* replication, macrophages were first infected with *Mtb* (MOI=1) (14 hours, 37C). Extracellular *Mtb* was then washed off prior to the addition of IgG from each individual patient (100µg/mL).

Luminescence was measured using a BioTek Synergy Neo2 Hybrid Multimode Reader plate reader every 24 hours until *Mtb* growth reached stationary phase. Each patient sample

was tested in duplicate in three independent experiments using macrophage derived from three different healthy HIV negative donors.

Statistics

Data are presented as median with 95% confidence intervals (Figure 1B-C, 4B,4D, Supplemental Figure 1, 3A). Data was analyzed by Mann – Whitney test (Table), Chi-square test (Table), logistic regression (Figure 1A), multiple linear regression to adjust for age and sex (Figure 1B-C, 4B, 4D, Supplemental Figure 1, 3A, 6) and to incorporate multiple antibody features (Figure 5C,5D, Supplemental Figure 7), Friedman test with adjustment for FDR using a two-stage step-up method of Benjamini, Krieger, and Yekutieli with Q=1% (Figure 2B, and Supplemental Figure 2D), principal components analysis (Figure 2C, 2D, 3A-B, Supplemental Figure 2E), hierarchical clustering (Supplemental Figure 2F), simple linear regression (Figure 5A, 5B, 6A, 6B, Supplemental Figure 5A-B), Pearson correlation (Supplemental Figure 4A), and unpaired t-test (Figure 6F) using STATA v16, Graphpad Prism10, and JMP17.2.0. Figures were generated using Graphpad Prism10, R using the ggplot package, Cytoscape v3.9.1, JMP17.2.0, and Biorender.

Data availability

Original data are available in the Supplemental Supporting Data file.

<u>Author contributions</u>

JM and PL designed and conducted experiments, acquired data, analyzed data, and wrote the manuscript. SB conducted experiments and acquired data. GA and JR provided reagents. BG conducted experiments, acquired data, analyzed data, provided reagents, and wrote the manuscript. BR designed the research study, provided reagents, and wrote the manuscript. LL

designed the research study, conducted experiments, acquired data, analyzed data, and wrote the manuscript.

Conflicts of interest

The authors have declared that no conflicts of interests exist.

Acknowledgements

We thank Gabrielle Lessen for her assistance with the in vitro *Mtb* macrophage infection experiments and manuscript editing. We thank Michael Shiloh for helpful comments. We thank study participants and clinical staff from the Secretaria de Salud de Tamaulipas and the Hidalgo Department of State and Health Services for field logistics support. This work is supported by UT Southwestern Disease Oriented Scholars Award (LLL), NIH NIAID 5R01AI158858 (LLL), NIH NIAID R21AI144541 (BIR), and NIH NIAID 5T32AI005284-44 (JRM).

References

1. Grobben M, Stuart RA, and van Gils MJ. The potential of engineered antibodies for HIV-1 therapy and cure. *Curr Opin Virol.* 2019;38:70-80.
2. Lu LL, Suscovich TJ, Fortune SM, and Alter G. Beyond binding: antibody effector functions in infectious diseases. *Nat Rev Immunol.* 2018;18(1):46-61.
3. Nunes-Alves C, Booty MG, Carpenter SM, Jayaraman P, Rothchild AC, and Behar SM. In search of a new paradigm for protective immunity to TB. *Nat Rev Microbiol.* 2014;12(4):289-99.
4. Carpenter SM, and Lu LL. Leveraging Antibody, B Cell and Fc Receptor Interactions to Understand Heterogeneous Immune Responses in Tuberculosis. *Front Immunol.* 2022;13:830482.
5. Grace PS, Gunn BM, and Lu LL. Engineering the supernatural: monoclonal antibodies for challenging infectious diseases. *Curr Opin Biotechnol.* 2022;78:102818.
6. Jacobs AJ, Mongkolsapaya J, Screaton GR, McShane H, and Wilkinson RJ. Antibodies and tuberculosis. *Tuberculosis (Edinb).* 2016;101:102-13.
7. Forget A, Benoit JC, Turcotte R, and Gusew-Chartrand N. Enhancement activity of anti-mycobacterial sera in experimental Mycobacterium bovis (BCG) infection in mice. *Infect Immun.* 1976;13(5):1301-6.

8. THE RESULTS OBTAINED BY DR. VIQUERAT IN HIS TREATMENT OF TUBERCULOSIS. *Lancet.* 1894;144(3709):756-7.
9. Glatman-Freedman A, and Casadevall A. Serum therapy for tuberculosis revisited: reappraisal of the role of antibody-mediated immunity against Mycobacterium tuberculosis. *Clin Microbiol Rev.* 1998;11(3):514-32.
10. Philips JA, and Ernst JD. Tuberculosis pathogenesis and immunity. *Annu Rev Pathol.* 2012;7:353-84.
11. Kauffman KD, Sakai S, Lora NE, Namasivayam S, Baker PJ, Kamenyeva O, et al. PD-1 blockade exacerbates Mycobacterium tuberculosis infection in rhesus macaques. *Sci Immunol.* 2021;6(55).
12. Ahmed M, Tezera LB, Elkington PT, and Leslie AJ. The paradox of immune checkpoint inhibition re-activating tuberculosis. *Eur Respir J.* 2022;60(5).
13. Fletcher HA, Snowden MA, Landry B, Rida W, Satti I, Harris SA, et al. T-cell activation is an immune correlate of risk in BCG vaccinated infants. *Nat Commun.* 2016;7:11290.
14. Nimmerjahn F, and Ravetch JV. Fcgamma receptors as regulators of immune responses. *Nat Rev Immunol.* 2008;8(1):34-47.
15. Vidarsson G, Dekkers G, and Rispens T. IgG subclasses and allotypes: from structure to effector functions. *Front Immunol.* 2014;5:520.
16. Bruhns P, Iannascoli B, England P, Mancardi DA, Fernandez N, Jorieux S, et al. Specificity and affinity of human Fcgamma receptors and their polymorphic variants for human IgG subclasses. *Blood.* 2009;113(16):3716-25.
17. Wang TT. IgG Fc Glycosylation in Human Immunity. *Curr Top Microbiol Immunol.* 2019;423:63-75.
18. Maglione PJ, Xu J, Casadevall A, and Chan J. Fc gamma receptors regulate immune activation and susceptibility during Mycobacterium tuberculosis infection. *J Immunol.* 2008;180(5):3329-38.
19. Roy Chowdhury R, Vallania F, Yang Q, Lopez Angel CJ, Darboe F, Penn-Nicholson A, et al. A multi-cohort study of the immune factors associated with M. tuberculosis infection outcomes. *Nature.* 2018;560(7720):644-8.
20. Lu LL, Chung AW, Rosebrock TR, Ghebremichael M, Yu WH, Grace PS, et al. A Functional Role for Antibodies in Tuberculosis. *Cell.* 2016;167(2):433-43 e14.
21. Lu LL, Das J, Grace PS, Fortune SM, Restrepo BI, and Alter G. Antibody Fc Glycosylation Discriminates Between Latent and Active Tuberculosis. *J Infect Dis.* 2020;222(12):2093-102.
22. Hermann C, and King CG. TB or not to be: what specificities and impact do antibodies have during tuberculosis? *Oxf Open Immunol.* 2021;2(1):iqab015.
23. Cho YS, Dobos KM, Prenni J, Yang H, Hess A, Rosenkrands I, et al. Deciphering the proteome of the in vivo diagnostic reagent "purified protein derivative" from Mycobacterium tuberculosis. *Proteomics.* 2012;12(7):979-91.
24. Yang H, Kruh-Garcia NA, and Dobos KM. Purified protein derivatives of tuberculin--past, present, and future. *FEMS Immunol Med Microbiol.* 2012;66(3):273-80.
25. Mukherjee J, Nussbaum G, Scharff MD, and Casadevall A. Protective and nonprotective monoclonal antibodies to Cryptococcus neoformans originating from one B cell. *J Exp Med.* 1995;181(1):405-9.

26. DiLillo DJ, Tan GS, Palese P, and Ravetch JV. Broadly neutralizing hemagglutinin stalk-specific antibodies require FcgammaR interactions for protection against influenza virus in vivo. *Nat Med.* 2014;20(2):143-51.
27. Brinkhaus M, Pannecoucke E, van der Kooi EJ, Bentlage AEH, Derksen NIL, Andries J, et al. The Fab region of IgG impairs the internalization pathway of FcRn upon Fc engagement. *Nat Commun.* 2022;13(1):6073.
28. Chen T, Blanc C, Liu Y, Ishida E, Singer S, Xu J, et al. Capsular glycan recognition provides antibody-mediated immunity against tuberculosis. *J Clin Invest.* 2020;130(4):1808-22.
29. Watson A, Li H, Ma B, Weiss R, Bendayan D, Abramovitz L, et al. Human antibodies targeting a Mycobacterium transporter protein mediate protection against tuberculosis. *Nat Commun.* 2021;12(1):602.
30. Zimmermann N, Thormann V, Hu B, Kohler AB, Imai-Matsushima A, Locht C, et al. Human isotype-dependent inhibitory antibody responses against Mycobacterium tuberculosis. *EMBO Mol Med.* 2016;8(11):1325-39.
31. Ishida E, Corrigan DT, Malonis RJ, Hofmann D, Chen T, Amin AG, et al. Monoclonal antibodies from humans with Mycobacterium tuberculosis exposure or latent infection recognize distinct arabinomannan epitopes. *Commun Biol.* 2021;4(1):1181.
32. Andrews JR, Noubary F, Walensky RP, Cerda R, Losina E, and Horsburgh CR. Risk of progression to active tuberculosis following reinfection with Mycobacterium tuberculosis. *Clin Infect Dis.* 2012;54(6):784-91.
33. Restrepo BI, Camerlin AJ, Rahbar MH, Wang W, Restrepo MA, Zarate I, et al. Cross-sectional assessment reveals high diabetes prevalence among newly-diagnosed tuberculosis cases. *Bull World Health Organ.* 2011;89(5):352-9.
34. Lewinsohn DM, Leonard MK, LoBue PA, Cohn DL, Daley CL, Desmond E, et al. Official American Thoracic Society/Infectious Diseases Society of America/Centers for Disease Control and Prevention Clinical Practice Guidelines: Diagnosis of Tuberculosis in Adults and Children. *Clin Infect Dis.* 2017;64(2):111-5.
35. Pai M, Denkinger CM, Kik SV, Rangaka MX, Zwerling A, Oxlade O, et al. Gamma interferon release assays for detection of Mycobacterium tuberculosis infection. *Clin Microbiol Rev.* 2014;27(1):3-20.
36. Dutt TS, Karger BR, Fox A, Youssef N, Dadhwal R, Ali MZ, et al. Mucosal exposure to non-tuberculous mycobacteria elicits B cell-mediated immunity against pulmonary tuberculosis. *Cell Rep.* 2022;41(11):111783.
37. Brandt L, Feino Cunha J, Weinreich Olsen A, Chilima B, Hirsch P, Appelberg R, et al. Failure of the Mycobacterium bovis BCG vaccine: some species of environmental mycobacteria block multiplication of BCG and induction of protective immunity to tuberculosis. *Infect Immun.* 2002;70(2):672-8.
38. Shah JA, Lindestam Arlehamn CS, Horne DJ, Sette A, and Hawn TR. Nontuberculous Mycobacteria and Heterologous Immunity to Tuberculosis. *J Infect Dis.* 2019;220(7):1091-8.
39. van Dorst M, Pyuza JJ, Nkurunungi G, Kullaya VI, Smits HH, Hogendoorn PCW, et al. Immunological factors linked to geographical variation in vaccine responses. *Nat Rev Immunol.* 2024;24(4):250-63.

40. Black GF, Dockrell HM, Crampin AC, Floyd S, Weir RE, Bliss L, et al. Patterns and implications of naturally acquired immune responses to environmental and tuberculous mycobacterial antigens in northern Malawi. *J Infect Dis.* 2001;184(3):322-9.
41. Cole ST, Brosch R, Parkhill J, Garnier T, Churcher C, Harris D, et al. Deciphering the biology of Mycobacterium tuberculosis from the complete genome sequence. *Nature.* 1998;393(6685):537-44.
42. Lucas M, Ryan JM, Watkins J, Early K, Kruh-Garcia NA, Mehaffy C, et al. Extraction and Separation of Mycobacterial Proteins. *Methods Mol Biol.* 2021;2314:77-107.
43. Hirschfield GR, McNeil M, and Brennan PJ. Peptidoglycan-associated polypeptides of Mycobacterium tuberculosis. *J Bacteriol.* 1990;172(2):1005-13.
44. Sonnenberg MG, and Belisle JT. Definition of Mycobacterium tuberculosis culture filtrate proteins by two-dimensional polyacrylamide gel electrophoresis, N-terminal amino acid sequencing, and electrospray mass spectrometry. *Infect Immun.* 1997;65(11):4515-24.
45. Perley CC, Frahm M, Click EM, Dobos KM, Ferrari G, Stout JE, et al. The human antibody response to the surface of Mycobacterium tuberculosis. *PLoS One.* 2014;9(2):e98938.
46. Li H, Wang XX, Wang B, Fu L, Liu G, Lu Y, et al. Latently and uninfected healthcare workers exposed to TB make protective antibodies against Mycobacterium tuberculosis. *Proc Natl Acad Sci U S A.* 2017;114(19):5023-8.
47. Weldingh K, and Andersen P. Immunological evaluation of novel Mycobacterium tuberculosis culture filtrate proteins. *FEMS Immunol Med Microbiol.* 1999;23(2):159-64.
48. Coppola M, and Ottenhoff TH. Genome wide approaches discover novel Mycobacterium tuberculosis antigens as correlates of infection, disease, immunity and targets for vaccination. *Semin Immunol.* 2018;39:88-101.
49. Belisle JT, Vissa VD, Sievert T, Takayama K, Brennan PJ, and Besra GS. Role of the major antigen of Mycobacterium tuberculosis in cell wall biogenesis. *Science.* 1997;276(5317):1420-2.
50. Renshaw PS, Lightbody KL, Veverka V, Muskett FW, Kelly G, Frenkiel TA, et al. Structure and function of the complex formed by the tuberculosis virulence factors CFP-10 and ESAT-6. *EMBO J.* 2005;24(14):2491-8.
51. McLellan JS, Ray WC, and Peeples ME. Structure and function of respiratory syncytial virus surface glycoproteins. *Curr Top Microbiol Immunol.* 2013;372:83-104.
52. World Health O. Geneva: World Health Organization; 2011.
53. Steingart KR, Flores LL, Dendukuri N, Schiller I, Laal S, Ramsay A, et al. Commercial serological tests for the diagnosis of active pulmonary and extrapulmonary tuberculosis: an updated systematic review and meta-analysis. *PLoS Med.* 2011;8(8):e1001062.
54. Jones MB, Oswald DM, Joshi S, Whiteheart SW, Orlando R, and Cobb BA. B-cell-independent sialylation of IgG. *Proc Natl Acad Sci U S A.* 2016;113(26):7207-12.

55. Schaffert A, Hanic M, Novokmet M, Zaytseva O, Kristic J, Lux A, et al. Minimal B Cell Extrinsic IgG Glycan Modifications of Pro- and Anti-Inflammatory IgG Preparations in vivo. *Front Immunol.* 2019;10:3024.
56. Grace PS, Dolatshahi S, Lu LL, Cain A, Palmieri F, Petrone L, et al. Antibody Subclass and Glycosylation Shift Following Effective TB Treatment. *Front Immunol.* 2021;12:679973.
57. Davies LRL, Wang C, Steigler P, Bowman KA, Fischinger S, Hatherill M, et al. Age and sex influence antibody profiles associated with tuberculosis progression. *Nat Microbiol.* 2024.
58. Lu LL, Smith MT, Yu KKQ, Luedemann C, Suscovich TJ, Grace PS, et al. IFN-gamma-independent immune markers of Mycobacterium tuberculosis exposure. *Nat Med.* 2019;25(6):977-87.
59. Ahmed M, Thirunavukkarasu S, Rosa BA, Thomas KA, Das S, Rangel-Moreno J, et al. Immune correlates of tuberculosis disease and risk translate across species. *Sci Transl Med.* 2020;12(528).
60. La Manna MP, Orlando V, Dieli F, Di Carlo P, Cascio A, Cuzzi G, et al. Quantitative and qualitative profiles of circulating monocytes may help identifying tuberculosis infection and disease stages. *PLoS One.* 2017;12(2):e0171358.
61. Vogelzang A, Lozza L, Reece ST, Perdomo C, Zedler U, Hahnke K, et al. Neonatal Fc Receptor Regulation of Lung Immunoglobulin and CD103+ Dendritic Cells Confers Transient Susceptibility to Tuberculosis. *Infect Immun.* 2016;84(10):2914-21.
62. Chen T, Blanc C, Eder AZ, Prados-Rosales R, Souza AC, Kim RS, et al. Association of Human Antibodies to Arabinomannan With Enhanced Mycobacterial Opsonophagocytosis and Intracellular Growth Reduction. *J Infect Dis.* 2016;214(2):300-10.
63. Liu Y, Chen T, Zhu Y, Furey A, Lowary TL, Chan J, et al. Features and protective efficacy of human mAbs targeting Mycobacterium tuberculosis arabinomannan. *JCI Insight.* 2023;8(20).
64. Kumar SK, Singh P, and Sinha S. Naturally produced opsonizing antibodies restrict the survival of Mycobacterium tuberculosis in human macrophages by augmenting phagosome maturation. *Open Biol.* 2015;5(12):150171.
65. Glickman MS, and Jacobs WR, Jr. Microbial pathogenesis of Mycobacterium tuberculosis: dawn of a discipline. *Cell.* 2001;104(4):477-85.
66. Chandra P, Grigsby SJ, and Philips JA. Immune evasion and provocation by Mycobacterium tuberculosis. *Nat Rev Microbiol.* 2022;20(12):750-66.
67. DesJardin LE, Kaufman TM, Potts B, Kutzbach B, Yi H, and Schlesinger LS. Mycobacterium tuberculosis-infected human macrophages exhibit enhanced cellular adhesion with increased expression of LFA-1 and ICAM-1 and reduced expression and/or function of complement receptors, FcgammaRII and the mannose receptor. *Microbiology (Reading).* 2002;148(Pt 10):3161-71.
68. Cohen SB, Gern BH, Delahaye JL, Adams KN, Plumlee CR, Winkler JK, et al. Alveolar Macrophages Provide an Early Mycobacterium tuberculosis Niche and Initiate Dissemination. *Cell Host Microbe.* 2018;24(3):439-46 e4.

69. Andreu N, Zelmer A, Fletcher T, Elkington PT, Ward TH, Ripoll J, et al. Optimisation of bioluminescent reporters for use with mycobacteria. *PLoS One.* 2010;5(5):e10777.
70. Irvine EB, Peters JM, Lu R, Grace PS, Sixsmith J, Wallace A, et al. Fc-engineered antibodies leverage neutrophils to drive control of Mycobacterium tuberculosis. *bioRxiv.* 2022:2022.05.01.490220.
71. Hoff DR, Ryan GJ, Driver ER, Ssemakulu CC, De Groote MA, Basaraba RJ, et al. Location of intra- and extracellular M. tuberculosis populations in lungs of mice and guinea pigs during disease progression and after drug treatment. *PLoS One.* 2011;6(3):e17550.
72. Hernandez-Pando R, Jeyanathan M, Mengistu G, Aguilar D, Orozco H, Harboe M, et al. Persistence of DNA from Mycobacterium tuberculosis in superficially normal lung tissue during latent infection. *Lancet.* 2000;356(9248):2133-8.
73. Damelang T, Rogerson SJ, Kent SJ, and Chung AW. Role of IgG3 in Infectious Diseases. *Trends Immunol.* 2019;40(3):197-211.
74. Shields RL, Lai J, Keck R, O'Connell LY, Hong K, Meng YG, et al. Lack of fucose on human IgG1 N-linked oligosaccharide improves binding to human Fcgamma RIII and antibody-dependent cellular toxicity. *J Biol Chem.* 2002;277(30):26733-40.
75. Ferrara C, Grau S, Jager C, Sondermann P, Brunker P, Waldhauer I, et al. Unique carbohydrate-carbohydrate interactions are required for high affinity binding between FcgammaRIII and antibodies lacking core fucose. *Proc Natl Acad Sci U S A.* 2011;108(31):12669-74.
76. Bates TA, Lu P, Kang YJ, Schoen D, Thornton M, McBride SK, et al. BNT162b2-induced neutralizing and non-neutralizing antibody functions against SARS-CoV-2 diminish with age. *Cell Rep.* 2022;41(4):111544.
77. Vattepu R, Sneed SL, and Anthony RM. Sialylation as an Important Regulator of Antibody Function. *Front Immunol.* 2022;13:818736.
78. Barry CE, 3rd, Boshoff HI, Dartois V, Dick T, Ehrt S, Flynn J, et al. The spectrum of latent tuberculosis: rethinking the biology and intervention strategies. *Nat Rev Microbiol.* 2009;7(12):845-55.
79. Burel JG, Wang W, Wuhrer M, Dedicoat M, Fletcher TE, Cunningham AF, et al. IgG glycosylation associates with risk of progression from latent to active tuberculosis. *J Infect.* 2024;88(3):106115.
80. Baumann R, Kaempfer S, Chegou NN, Nene NF, Veenstra H, Spallek R, et al. Serodiagnostic markers for the prediction of the outcome of intensive phase tuberculosis therapy. *Tuberculosis (Edinb).* 2013;93(2):239-45.
81. Fischinger S, Cizmeci D, Shin S, Davies L, Grace PS, Sivro A, et al. A Mycobacterium tuberculosis Specific IgG3 Signature of Recurrent Tuberculosis. *Front Immunol.* 2021;12:729186.
82. Bitencourt J, Peralta-Alvarez MP, Wilkie M, Jacobs A, Wright D, Salman Almujri S, et al. Induction of Functional Specific Antibodies, IgG-Secreting Plasmablasts and Memory B Cells Following BCG Vaccination. *Front Immunol.* 2021;12:798207.

83. Moliva JI, Turner J, and Torrelles JB. Immune Responses to Bacillus Calmette-Guerin Vaccination: Why Do They Fail to Protect against Mycobacterium tuberculosis? *Front Immunol.* 2017;8:407.
84. Tran AC, Diogo GR, Paul MJ, Copland A, Hart P, Mehta N, et al. Mucosal Therapy of Multi-Drug Resistant Tuberculosis With IgA and Interferon-gamma. *Front Immunol.* 2020;11:582833.
85. Krishnananthasivam S, Li H, Bouzeyen R, Shunmuganathan B, Purushotorman K, Liao X, et al. An anti-LpqH human monoclonal antibody from an asymptomatic individual mediates protection against Mycobacterium tuberculosis. *NPJ Vaccines.* 2023;8(1):127.
86. Bournazos S, Gupta A, and Ravetch JV. The role of IgG Fc receptors in antibody-dependent enhancement. *Nat Rev Immunol.* 2020;20(10):633-43.
87. Halstead SB, Mahalingam S, Marovich MA, Ubol S, and Mosser DM. Intrinsic antibody-dependent enhancement of microbial infection in macrophages: disease regulation by immune complexes. *Lancet Infect Dis.* 2010;10(10):712-22.
88. Torres VVL, Coggon CF, and Wells TJ. Antibody-Dependent Enhancement of Bacterial Disease: Prevalence, Mechanisms, and Treatment. *Infect Immun.* 2021;89(4).
89. Kuzmina NA, Younan P, Gilchuk P, Santos RI, Flyak AI, Ilinykh PA, et al. Antibody-Dependent Enhancement of Ebola Virus Infection by Human Antibodies Isolated from Survivors. *Cell Rep.* 2018;24(7):1802-15 e5.
90. Widen RH, Newton CA, Klein TW, and Friedman H. Antibody-mediated enhancement of Legionella pneumophila-induced interleukin 1 activity. *Infect Immun.* 1993;61(10):4027-32.
91. Miles SA, Conrad SM, Alves RG, Jeronimo SM, and Mosser DM. A role for IgG immune complexes during infection with the intracellular pathogen Leishmania. *J Exp Med.* 2005;201(5):747-54.
92. Kima PE, Constant SL, Hannum L, Colmenares M, Lee KS, Haberman AM, et al. Internalization of Leishmania mexicana complex amastigotes via the Fc receptor is required to sustain infection in murine cutaneous leishmaniasis. *J Exp Med.* 2000;191(6):1063-8.
93. Brodin P, de Jonge MI, Majlessi L, Leclerc C, Nilges M, Cole ST, et al. Functional analysis of early secreted antigenic target-6, the dominant T-cell antigen of Mycobacterium tuberculosis, reveals key residues involved in secretion, complex formation, virulence, and immunogenicity. *J Biol Chem.* 2005;280(40):33953-9.
94. Stanley SA, Raghavan S, Hwang WW, and Cox JS. Acute infection and macrophage subversion by Mycobacterium tuberculosis require a specialized secretion system. *Proc Natl Acad Sci U S A.* 2003;100(22):13001-6.
95. Bates TA, Trank-Greene M, Nguyenla X, Anastas A, Gurmessa SK, Merutka IR, et al. ESAT-6 undergoes self-association at phagosomal pH and an ESAT-6 specific nanobody restricts M. tuberculosis growth in macrophages. *bioRxiv.* 2024.
96. Mehaffy C, Ryan JM, Kruh-Garcia NA, and Dobos KM. Extracellular Vesicles in Mycobacteria and Tuberculosis. *Front Cell Infect Microbiol.* 2022;12:912831.
97. Liu C, Zhao Z, Fan J, Lyon CJ, Wu HJ, Nedelkov D, et al. Quantification of circulating Mycobacterium tuberculosis antigen peptides allows rapid diagnosis of

active disease and treatment monitoring. *Proc Natl Acad Sci U S A.* 2017;114(15):3969-74.

98. Gunn BM, Lu R, Slein MD, Ilinykh PA, Huang K, Atyeo C, et al. A Fc engineering approach to define functional humoral correlates of immunity against Ebola virus. *Immunity.* 2021;54(4):815-28 e5.

99. Taborda CP, Rivera J, Zaragoza O, and Casadevall A. More is not necessarily better: prozone-like effects in passive immunization with IgG. *J Immunol.* 2003;170(7):3621-30.

100. Jurado RL, Campbell J, and Martin PD. Prozone phenomenon in secondary syphilis. Has its time arrived? *Arch Intern Med.* 1993;153(21):2496-8.

101. Goodner K, and Horsfall FL. The Protective Action of Type I Antipneumococcus Serum in Mice : Iv. The Prozone. *J Exp Med.* 1936;64(3):369-75.

102. Musvosvi M, Huang H, Wang C, Xia Q, Rozot V, Krishnan A, et al. T cell receptor repertoires associated with control and disease progression following Mycobacterium tuberculosis infection. *Nat Med.* 2023;29(1):258-69.

103. Lin PL, and Flynn JL. Understanding latent tuberculosis: a moving target. *J Immunol.* 2010;185(1):15-22.

104. Kunnath-Velayudhan S, Salamon H, Wang HY, Davidow AL, Molina DM, Huynh VT, et al. Dynamic antibody responses to the Mycobacterium tuberculosis proteome. *Proc Natl Acad Sci U S A.* 2010;107(33):14703-8.

105. Wanchu A, Dong Y, Sethi S, Myneedu VP, Nadas A, Liu Z, et al. Biomarkers for clinical and incipient tuberculosis: performance in a TB-endemic country. *PLoS One.* 2008;3(4):e2071.

106. Irvine EB, O'Neil A, Darrah PA, Shin S, Choudhary A, Li W, et al. Robust IgM responses following intravenous vaccination with Bacille Calmette-Guerin associate with prevention of Mycobacterium tuberculosis infection in macaques. *Nat Immunol.* 2021;22(12):1515-23.

107. Balu S, Reljic R, Lewis MJ, Pleass RJ, McIntosh R, van Kooten C, et al. A novel human IgA monoclonal antibody protects against tuberculosis. *J Immunol.* 2011;186(5):3113-9.

108. Ishida E, Corrigan DT, Chen T, Liu Y, Kim RS, Song L, et al. Mucosal and systemic antigen-specific antibody responses correlate with protection against active tuberculosis in nonhuman primates. *EBioMedicine.* 2024;99:104897.

109. Dijkman K, Aguilo N, Boot C, Hofman SO, Sombroek CC, Vervenne RAW, et al. Pulmonary MTBVAC vaccination induces immune signatures previously correlated with prevention of tuberculosis infection. *Cell Rep Med.* 2021;2(1):100187.

110. Scully EP. Sex, gender and infectious disease. *Nat Microbiol.* 2022;7(3):359-60.

111. Oni T, Berkowitz N, Kubjane M, Goliath R, Levitt NS, and Wilkinson RJ. Trilateral overlap of tuberculosis, diabetes and HIV-1 in a high-burden African setting: implications for TB control. *Eur Respir J.* 2017;50(1).

112. van Woudenbergh E, Irvine EB, Davies L, de Kock M, Hanekom WA, Day CL, et al. HIV Is Associated with Modified Humoral Immune Responses in the Setting of HIV/TB Coinfection. *mSphere.* 2020;5(3).

113. Restrepo BI. Diabetes and Tuberculosis. *Microbiol Spectr.* 2016;4(6).

114. Tanigaki K, Sacharidou A, Peng J, Chambliss KL, Yuhanna IS, Ghosh D, et al. Hyposialylated IgG activates endothelial IgG receptor FcgammaRIIB to promote obesity-induced insulin resistance. *J Clin Invest.* 2018;128(1):309-22.
115. Haycroft ER, Damelang T, Lopez E, Rodgers MA, Wines BD, Hogarth M, et al. Antibody glycosylation correlates with disease progression in SIV-Mycobacterium tuberculosis coinfected cynomolgus macaques. *Clin Transl Immunology.* 2023;12(11):e1474.
116. Ronacher K, Joosten SA, van Crevel R, Dockrell HM, Walzl G, and Ottenhoff TH. Acquired immunodeficiencies and tuberculosis: focus on HIV/AIDS and diabetes mellitus. *Immunol Rev.* 2015;264(1):121-37.
117. Ahangarzadeh S, Bandehpour M, and Kazemi B. Selection of single-chain variable fragments specific for Mycobacterium tuberculosis ESAT-6 antigen using ribosome display. *Iran J Basic Med Sci.* 2017;20(3):327-33.
118. Brown EP, Licht AF, Dugast AS, Choi I, Bailey-Kellogg C, Alter G, et al. High-throughput, multiplexed IgG subclassing of antigen-specific antibodies from clinical samples. *J Immunol Methods.* 2012;386(1-2):117-23.
119. Adhikari EH, Lu P, Kang YJ, McDonald AR, Pruszynski JE, Bates TA, et al. Diverging Maternal and Cord Antibody Functions From SARS-CoV-2 Infection and Vaccination in Pregnancy. *J Infect Dis.* 2024;229(2):462-72.
120. Mahan AE, Tedesco J, Dionne K, Baruah K, Cheng HD, De Jager PL, et al. A method for high-throughput, sensitive analysis of IgG Fc and Fab glycosylation by capillary electrophoresis. *J Immunol Methods.* 2015;417:34-44.
121. Varadi C, Lew C, and Guttman A. Rapid magnetic bead based sample preparation for automated and high throughput N-glycan analysis of therapeutic antibodies. *Anal Chem.* 2014;86(12):5682-7.
122. Brown EP, Dowell KG, Boesch AW, Normandin E, Mahan AE, Chu T, et al. Multiplexed Fc array for evaluation of antigen-specific antibody effector profiles. *J Immunol Methods.* 2017;443:33-44.
123. Neuber T, Frese K, Jaehrling J, Jager S, Daubert D, Felderer K, et al. Characterization and screening of IgG binding to the neonatal Fc receptor. *MAbs.* 2014;6(4):928-42.
124. Ackerman ME, Moldt B, Wyatt RT, Dugast AS, McAndrew E, Tsoukas S, et al. A robust, high-throughput assay to determine the phagocytic activity of clinical antibody samples. *J Immunol Methods.* 2011;366(1-2):8-19.
125. Darrah PA, Patel DT, De Luca PM, Lindsay RW, Davey DF, Flynn BJ, et al. Multifunctional TH1 cells define a correlate of vaccine-mediated protection against Leishmania major. *Nat Med.* 2007;13(7):843-50.
126. Jegaskanda S, Job ER, Kramski M, Laurie K, Isitman G, de Rose R, et al. Cross-reactive influenza-specific antibody-dependent cellular cytotoxicity antibodies in the absence of neutralizing antibodies. *J Immunol.* 2013;190(4):1837-48.

Table. Cohort characteristics

	Latent TB	Active TB	Significance	Endemic Controls
Total number of individuals	18	19		8
Age in years (range [median])	23 – 79 (40)	18 – 82 (38)	$P = 0.5730^{A}$	30 – 65 (47)
Sex (no. [%])			$P = 0.6185^{B}$	
Female	10 (56%)	9 (47%)		5 (63%)
Male	8 (44%)	10 (53%)		3 (38%)
BCG vaccination	15 (83%)	16 (84%)	$P = 0.9423^{C}$	7 (88%)

[A]Mann-Whitney U test was used to compare ages between latent and active TB groups. [B,C]Chi-square test was used to test the frequency of each sex and the rate of BCG vaccination between latent and active TB groups.

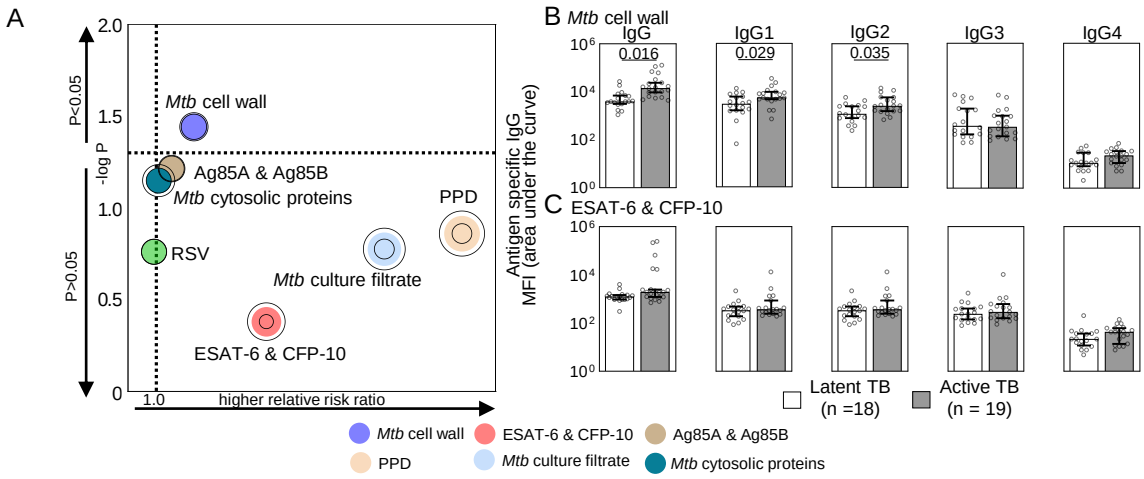

Figure 1. Differences between latent and active TB IgG titers are determined by antigen specificity. (A) The bubble plot shows the capacity of each antigen specific IgG to predict active TB disease and latent TB infection. Relative risk ratios (RRR) determined by logistic regression depict higher likelihood of active TB when >1 and latent TB when <1. Concentric rings represent 95% CI. **(B and C)** The median and 95% CI of the relative levels of IgG for the **(B)** most (*Mtb* cell wall) and **(C)** least (ESAT-6 & CFP-10) significant antigens in **(A)** are shown with *P*-values adjusted for sex and age using linear regression where $P \leq 0.05$ was considered significant.

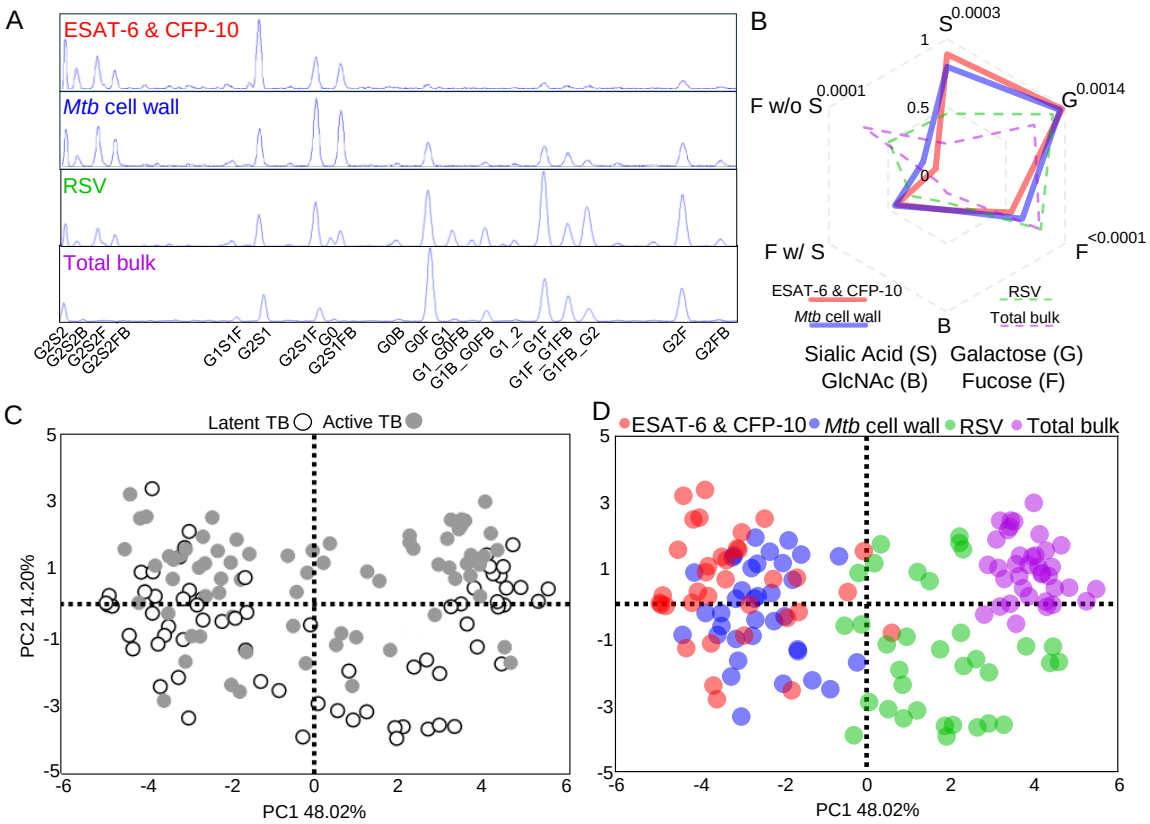

Figure 2. Antigen specificity separates antibody Fc domain glycosylation in latent and active TB. (A) Chromatograms depict the relative abundance of individual glycoforms isolated from the Fc domain of antigen specific and bulk total IgG from a representative individual TB patient. **(B)** Radar plot shows the median of the relative abundance of total glycans from antigen specific and total bulk IgG. Comparisons between *Mtb* antigens are made by Wilcoxon matched-pairs signed-ranks tests and *P*-values adjusted for multiple comparisons by controlling for the false discovery rate (Q=1%) using the two-stage step-up method of Benjamini, Krieger, Yekutieli. Adjusted *P*-values <0.05 comparing ESAT-6 & CFP-10 and *Mtb* cell wall are shown. The score plot from principal components analysis with each dot summarizing the linear combination of antigen specific glycoforms for each individual patient (n=37 patients) is shown with markers identified by **(C)** latent and active TB and **(D)** antigen specificity.

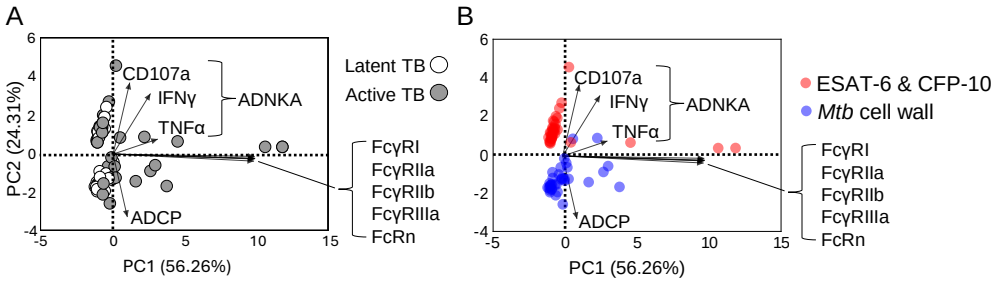

Figure 3. Antibody Fc effector functions diverge more by antigen specificity than latent and active TB. Biplots show scores and loadings from principal components analysis with each dot summarizing the linear combination of the antigen specific IgG effector functions and FcR binding for each individual TB patient (n=37 patients) with markers identified by **(A)** latent and active TB and **(B)** antigen specificity. The loadings (arrows) show the coefficients of the linear combination of the Fc effector functions (antibody dependent natural killer cell activation (ADNKA), Fc receptor binding, and antibody dependent cellular phagocytosis (ADCP)) from which the principal components are constructed, demonstrating which IgG features contribute to the components.

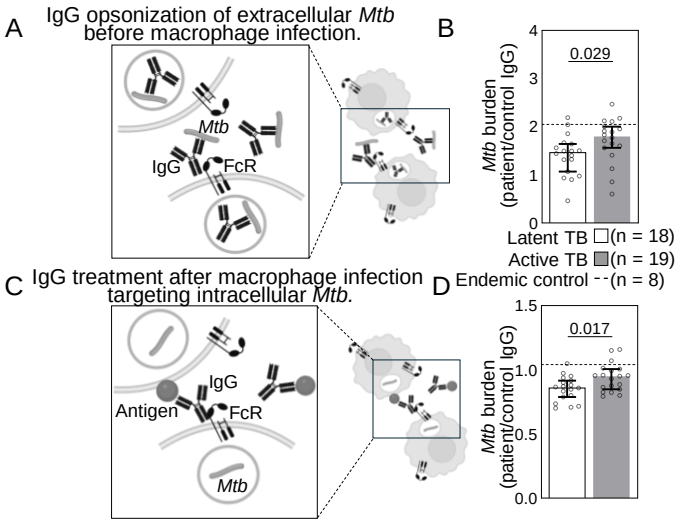

Figure 4. Latent and active TB IgG differentially impact extracellular and intracellular *Mtb* in macrophage infection. (A) To test the effect of antibodies on extracellular *Mtb*, a H37Rv luminescent reporter strain opsonized by IgG isolated from each patient was used to infect primary monocyte derived macrophages (pMDMs) at an MOI=1. Daily luminescence readings during the exponential phase growth were used to calculate burdens for extracellular *Mtb* **(B). (C)** To test the effect of antibodies on intracellular *Mtb*, human pMDMs were first infected with the H37Rv luminescent reporter strain, extracellular bacteria washed away, and then *Mtb* infected macrophages were treated with IgG. Daily luminescence readings during the exponential phase growth were used to calculate burdens for intracellular *Mtb* **(D)**. Each dot represents IgG from a TB patient and is the average of data from three independent experiments with three different macrophage donors. Median and 95% CI are shown. The dashed line shows the median of endemic controls. *P*-values are adjusted for sex and age using linear regression.

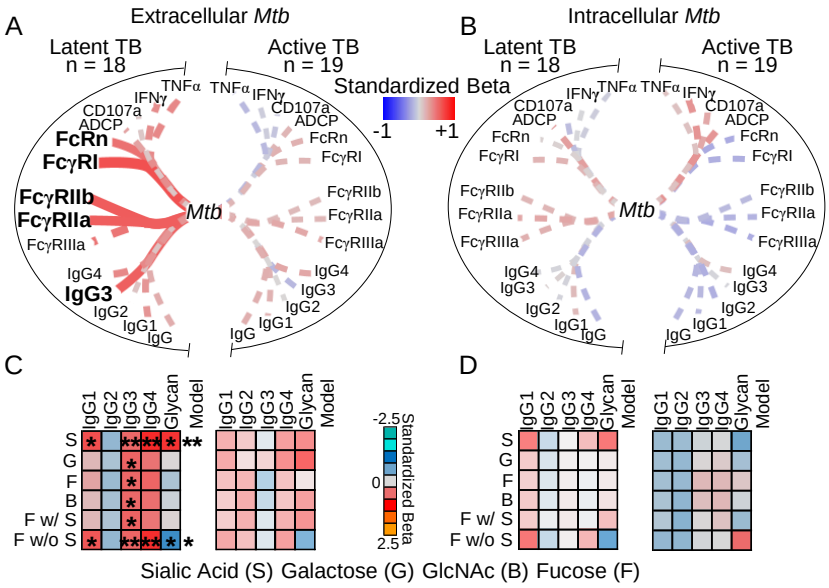

Figure 5. *Mtb* cell wall IgG enhances opsonophagocytosis of extracellular *Mtb*. Depicted is the dependence of *Mtb* burden after IgG treatment of **(A)** extracellular *Mtb* before infection for opsonophagocytosis into macrophages and **(B)** intracellular *Mtb* in macrophages after infection on *Mtb* cell wall IgG features from individuals with TB (n=37) as determined by simple linear regression. Line thickness is inversely proportional to the *P*-value. Solid lines denote $P \leq 0.05$; dashed $P > 0.05$. **(C and D)** Heatmaps depict the dependence of extracellular *Mtb* **(C)** and intracellular *Mtb* **(D)** burden on *Mtb* cell wall IgG subclasses and glycans together as determined by multiple linear regression. Colors represent the standardized beta for each variable and the model. *$P \leq 0.05$, **$P \leq 0.01$.

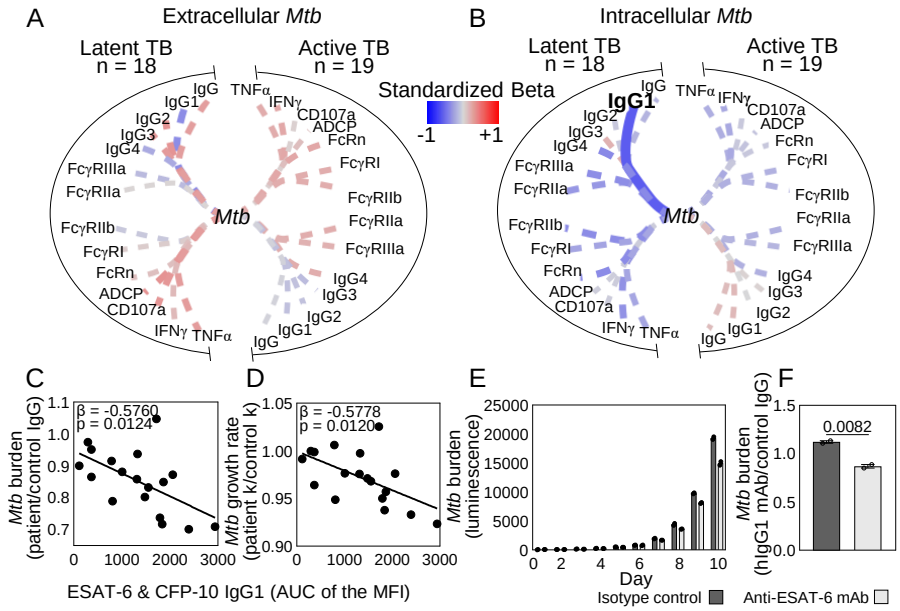

Figure 6. ESAT-6 & CFP-10 IgG inhibits intracellular *Mtb*. Depicted is the dependence of *Mtb* burden after IgG treatment of **(A)** extracellular *Mtb* before infection for opsonophagocytosis into macrophages and **(B)** intracellular *Mtb* in macrophages after infection on ESAT-6 & CFP-10 IgG features from individuals with TB (n=37) as determined by simple linear regression. Line thickness is inversely proportional to the *P*-value. Solid lines denote $P \leq 0.05$; dashed $P > 0.05$. Colors represent the standardized beta for each variable and the model. The dependence of intracellular *Mtb* **(C)** burden and **(D)** growth rate on ESAT-6 & CFP-10 IgG1 is plotted with each dot representing an individual with latent TB. **(E)** Columns show intracellular *Mtb* burden after treatment with a monoclonal hIgG1 reactive to ESAT-6 & CFP-10 (anti-ESAT-6 mAb) and isotype control CR3022 hIgG1 each day of infection. Mean and SEM are shown. **(F)** *Mtb* burden for monoclonal IgG relative to control polyclonal human IgG is quantitated and unpaired t-test was used to test significance. $P \leq 0.05$ was considered significant.

Table. Cohort characteristics

	Latent TB	Active TB	Significance	Endemic Controls
Total number of individuals	18	19		8
Age in years (range [median])	23 – 79 (40)	18 – 82 (38)	$P = 0.5730^{A}$	30 – 65 (47)
Sex (no. [%])			$P = 0.6185^{B}$	
Female	10 (56%)	9 (47%)		5 (63%)
Male	8 (44%)	10 (53%)		3 (38%)
BCG vaccination	15 (83%)	16 (84%)	$P = 0.9423^{C}$	7 (88%)

[A]Mann-Whitney U test was used to compare ages between latent and active TB groups. [B,C]Chi-square test was used to test the frequency of each sex and the rate of BCG vaccination between latent and active TB groups.

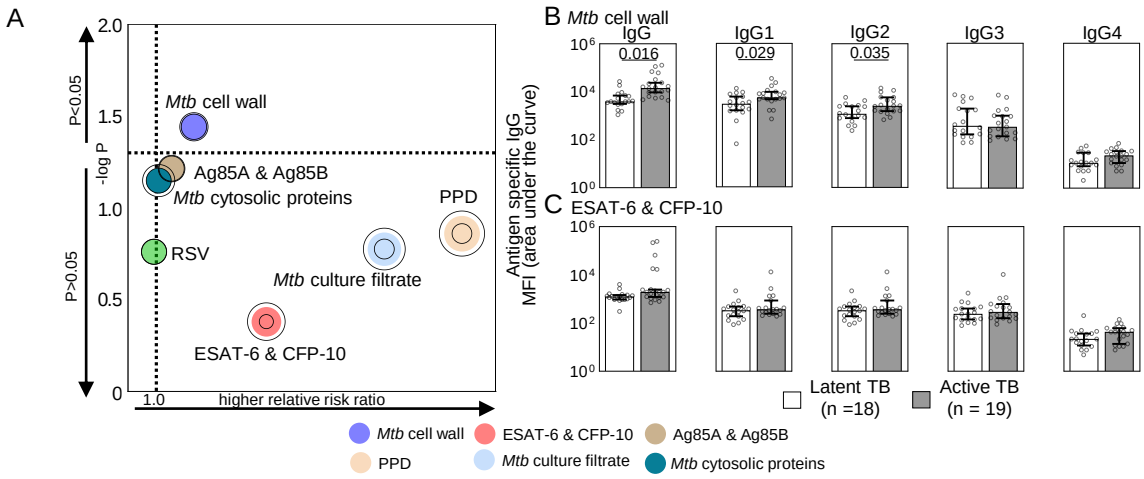

Figure 1. Differences between latent and active TB IgG titers are determined by antigen specificity. (A) The bubble plot shows the capacity of each antigen specific IgG to predict active TB disease and latent TB infection. Relative risk ratios (RRR) determined by logistic regression depict higher likelihood of active TB when >1 and latent TB when <1. Concentric rings represent 95% CI. **(B and C)** The median and 95% CI of the relative levels of IgG for the **(B)** most (*Mtb* cell wall) and **(C)** least (ESAT-6 & CFP-10) significant antigens in **(A)** are shown with *P*-values adjusted for sex and age using linear regression where $P \leq 0.05$ was considered significant.

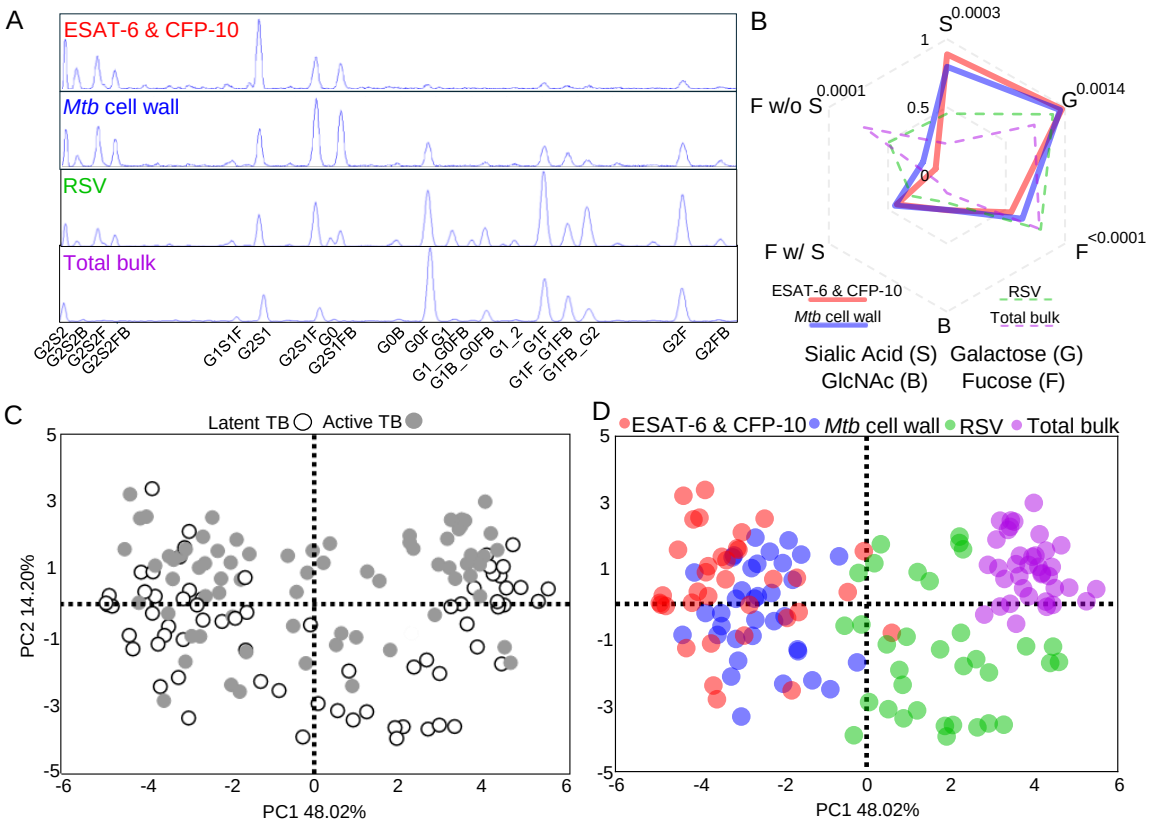

Figure 2. Antigen specificity separates antibody Fc domain glycosylation in latent and active TB. (A) Chromatograms depict the relative abundance of individual glycoforms isolated from the Fc domain of antigen specific and bulk total IgG from a representative individual TB patient. **(B)** Radar plot shows the median of the relative abundance of total glycans from antigen specific and total bulk IgG. Comparisons between *Mtb* antigens are made by Wilcoxon matched-pairs signed-ranks tests and *P*-values adjusted for multiple comparisons by controlling for the false discovery rate (Q=1%) using the two-stage step-up method of Benjamini, Krieger, Yekutieli. Adjusted *P*-values <0.05 comparing ESAT-6 & CFP-10 and *Mtb* cell wall are shown. The score plot from principal components analysis with each dot summarizing the linear combination of antigen specific glycoforms for each individual patient (n=37 patients) is shown with markers identified by **(C)** latent and active TB and **(D)** antigen specificity.

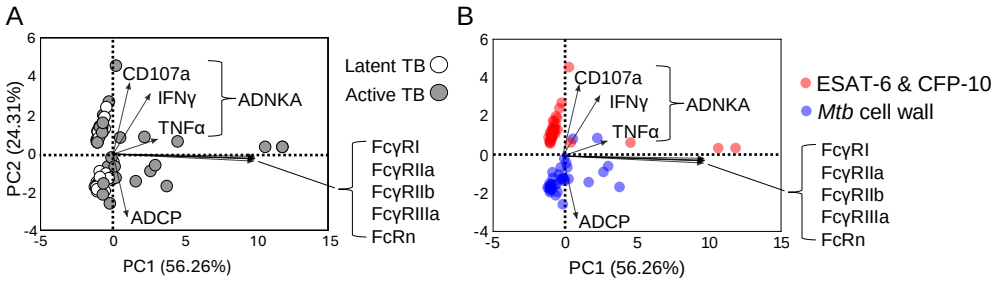

Figure 3. Antibody Fc effector functions diverge more by antigen specificity than latent and active TB. Biplots show scores and loadings from principal components analysis with each dot summarizing the linear combination of the antigen specific IgG effector functions and FcR binding for each individual TB patient (n=37 patients) with markers identified by **(A)** latent and active TB and **(B)** antigen specificity. The loadings (arrows) show the coefficients of the linear combination of the Fc effector functions (antibody dependent natural killer cell activation (ADNKA), Fc receptor binding, and antibody dependent cellular phagocytosis (ADCP)) from which the principal components are constructed, demonstrating which IgG features contribute to the components.

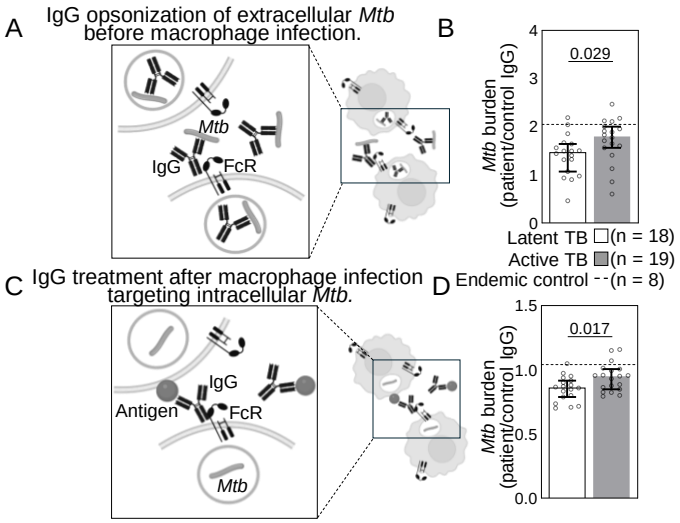

Figure 4. Latent and active TB IgG differentially impact extracellular and intracellular *Mtb* in macrophage infection. (A) To test the effect of antibodies on extracellular *Mtb*, a H37Rv luminescent reporter strain opsonized by IgG isolated from each patient was used to infect primary monocyte derived macrophages (pMDMs) at an MOI=1. Daily luminescence readings during the exponential phase growth were used to calculate burdens for extracellular *Mtb* **(B). (C)** To test the effect of antibodies on intracellular *Mtb*, human pMDMs were first infected with the H37Rv luminescent reporter strain, extracellular bacteria washed away, and then *Mtb* infected macrophages were treated with IgG. Daily luminescence readings during the exponential phase growth were used to calculate burdens for intracellular *Mtb* **(D)**. Each dot represents IgG from a TB patient and is the average of data from three independent experiments with three different macrophage donors. Median and 95% CI are shown. The dashed line shows the median of endemic controls. *P*-values are adjusted for sex and age using linear regression.

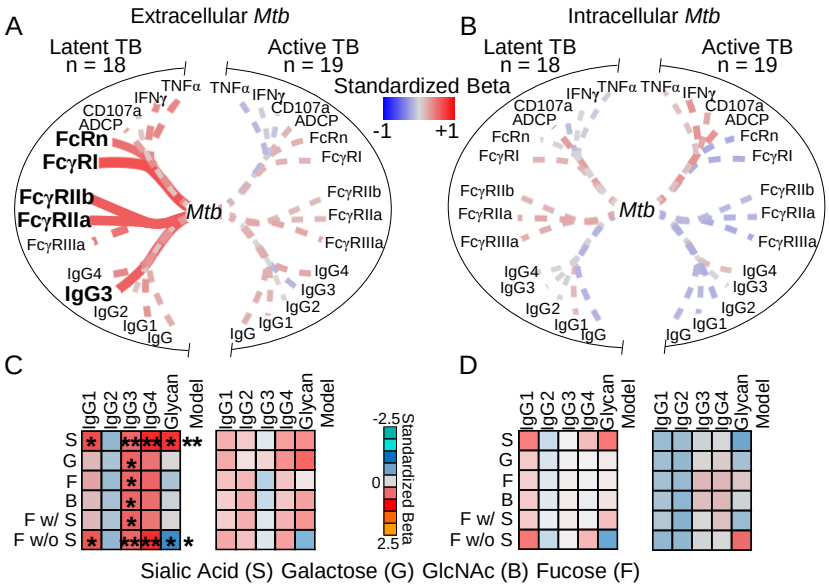

Figure 5. *Mtb* cell wall IgG enhances opsonophagocytosis of extracellular *Mtb*. Depicted is the dependence of *Mtb* burden after IgG treatment of **(A)** extracellular *Mtb* before infection for opsonophagocytosis into macrophages and **(B)** intracellular *Mtb* in macrophages after infection on *Mtb* cell wall IgG features from individuals with TB (n=37) as determined by simple linear regression. Line thickness is inversely proportional to the *P*-value. Solid lines denote $P \leq 0.05$; dashed $P > 0.05$. **(C and D)** Heatmaps depict the dependence of extracellular *Mtb* **(C)** and intracellular *Mtb* **(D)** burden on *Mtb* cell wall IgG subclasses and glycans together as determined by multiple linear regression. Colors represent the standardized beta for each variable and the model. *$P \leq 0.05$, **$P \leq 0.01$.

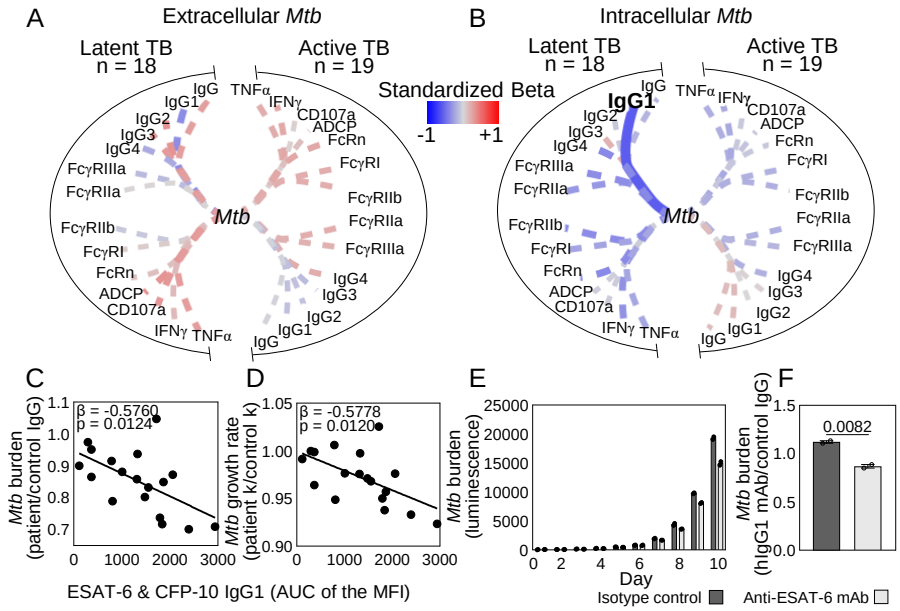

Figure 6. ESAT-6 & CFP-10 IgG inhibits intracellular *Mtb*. Depicted is the dependence of *Mtb* burden after IgG treatment of **(A)** extracellular *Mtb* before infection for opsonophagocytosis into macrophages and **(B)** intracellular *Mtb* in macrophages after infection on ESAT-6 & CFP-10 IgG features from individuals with TB (n=37) as determined by simple linear regression. Line thickness is inversely proportional to the *P*-value. Solid lines denote $P \leq 0.05$; dashed $P > 0.05$. Colors represent the standardized beta for each variable and the model. The dependence of intracellular *Mtb* **(C)** burden and **(D)** growth rate on ESAT-6 & CFP-10 IgG1 is plotted with each dot representing an individual with latent TB. **(E)** Columns show intracellular *Mtb* burden after treatment with a monoclonal hIgG1 reactive to ESAT-6 & CFP-10 (anti-ESAT-6 mAb) and isotype control CR3022 hIgG1 each day of infection. Mean and SEM are shown. **(F)** *Mtb* burden for monoclonal IgG relative to control polyclonal human IgG is quantitated and unpaired t-test was used to test significance. $P \leq 0.05$ was considered significant.

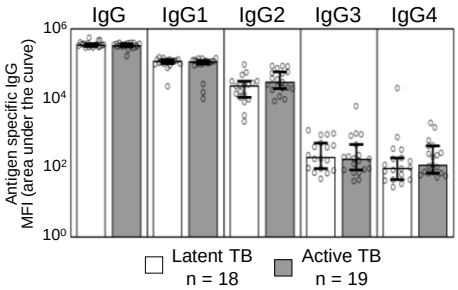

Supplemental Figure 1. No difference in RSV-specific IgG and subclasses between latent and active TB. Bar graphs show the median of the relative abundance of IgG for control RSV with 95% CI for individuals with latent and active TB. Statistical significance was determined by linear regression to adjust for sex and age. No *P*-values were ≤ 0.05.

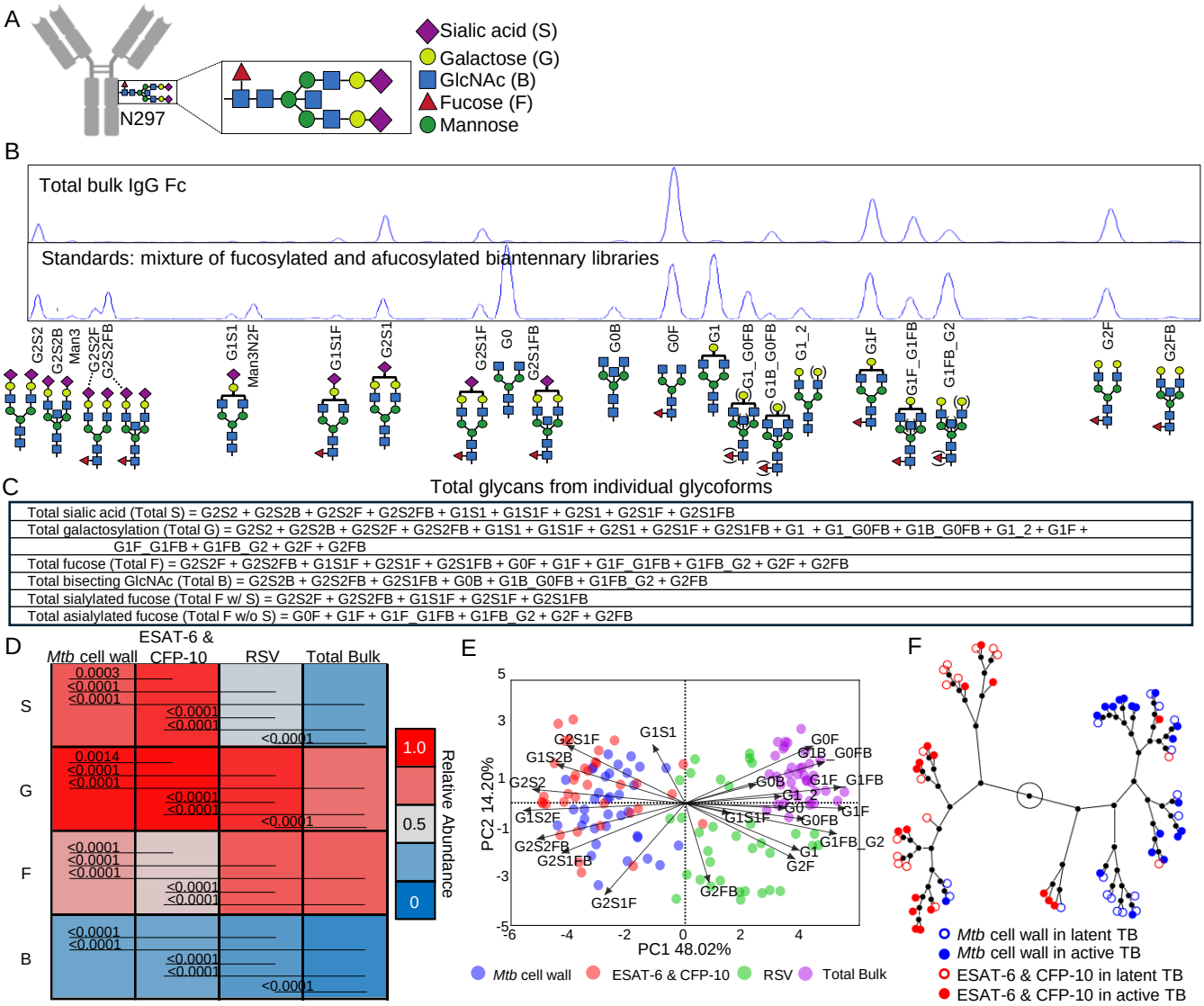

Supplemental Figure 2. Antigen specificity impacts IgG Fc domain N-glycosylation. (A) On a conserved N297 of the IgG Fc domain is a complex biantennary glycan structure composed of core mannose and N-acetylglucosamine on which variable amounts of galactose, sialic acid, and fucose are added. **(B)** Individual glycoforms on polyclonal IgG can be quantified by capillary electrophoresis using standards from biantennary glycan libraries. **(C)** Total glycans summarize individual glycoforms. **(D)** Heatmap shows the relative abundance of the glycans by antigen specificity with significance determined by Wilcoxon matched-pairs signed rank tests and *P*-values adjusted for multiple comparisons by controlling for the false discovery rate (Q=1%) using the two-stage step-up method of Benjamini, Krieger, Yekutieli. **(E)** Principal components analysis of individual IgG glycoforms from TB patients show separation by antigen specificities. Each dot summarizes the linear combination of antigen specific glycoforms of an individual patient. The loadings (arrows) show the coefficients of the linear combination of the individual glycoforms from which the principal components are constructed, demonstrating which individual glycoforms give the largest contribution to the components. **(F)** Constellation plot shows the relationships from hierarchical clustering of the glycan patterns for ESAT6 & CFP10 and *Mtb* cell wall IgG in latent and active TB.

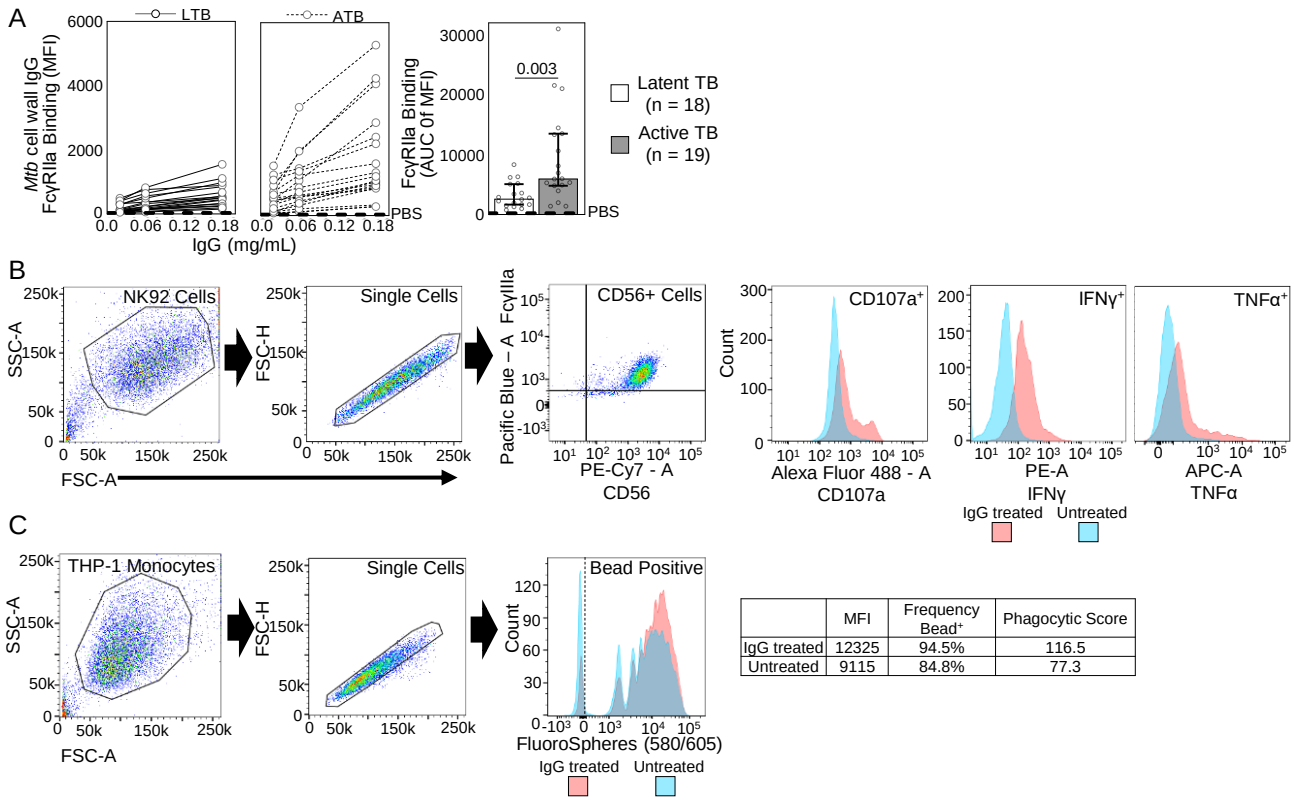

	MFI	Frequency Bead+	Phagocytic Score
IgG treated	12325	94.5%	116.5
Untreated	9115	84.8%	77.3

Supplemental Figure 3. High throughput approaches quantify antigen specific FcR binding and Fc effector functions in IgG isolated from individuals with TB. (A) Customized Luminex assays were used to measure the relative antigen specific IgG-FcγR binding in each patient sample across three dilutions to enhance sensitivity. A representative plot of the data is shown. Each line represents a single patient sample. The AUC of the MFI from IgG dilutions is used to summarize relative binding for each patient sample. The bold dashed line represents PBS control. Bar graphs show the median of with 95% CI for latent and active TB. Statistical significance was determined by linear regression to adjust for sex and age. **(B)** High throughput flow cytometry is used to measure antigen specific antibody dependent NK cell activation (ADNKA) in each individual patient sample. %NK CD56$^+$ cells expressing CD107a, IFNγ, or TNFα mark activation in response to antigen specific IgG. **(C)** The human monocyte cell line THP-1 is used to quantitate antibody dependent cellular phagocytosis (ADCP) by determining the frequency and extent of antibody mediated uptake of antigen coated coated fluorescent beads.

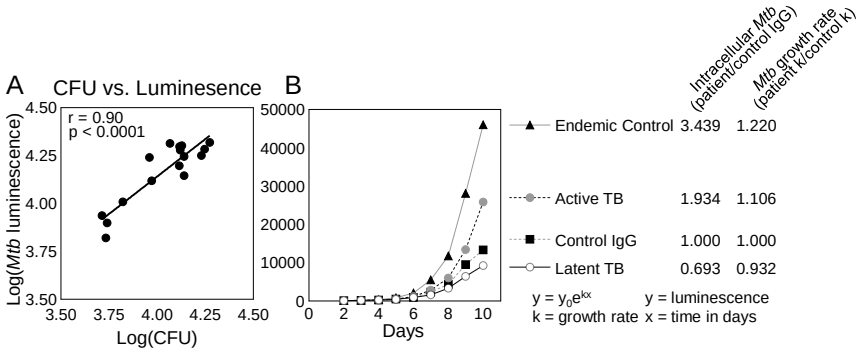

Supplemental Figure 4. Infection of macrophages by reporter strain of H37Rv captures differences in bacterial growth with treatment by latent and active TB IgG. (A) Log(*Mtb* luminescence) and Log(CFU) correlate as shown by Pearson. **(B)** Daily luminescence measurements of *Mtb* infected macrophages enable the determination of bacterial burden and growth rate by the exponential growth model.

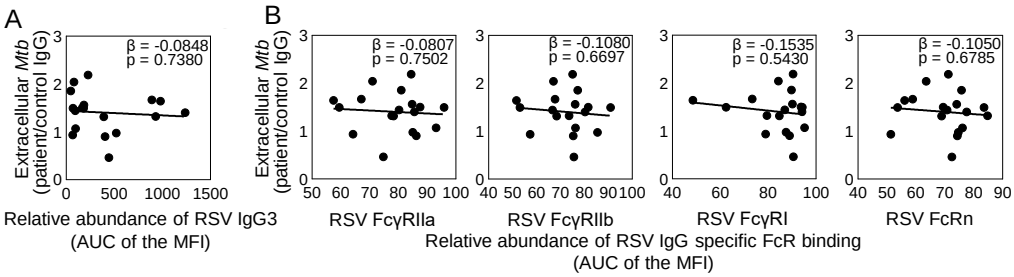

Supplemental Figure 5. RSV IgG3 and Fc receptor binding do not relate to extracellular *Mtb*. The absence of relationships between RSV IgG3 from latent TB and **(A)** *Mtb* burden and **(B)** Fc receptor binding as determined by simple linear regression is shown with no significant *P*-values.

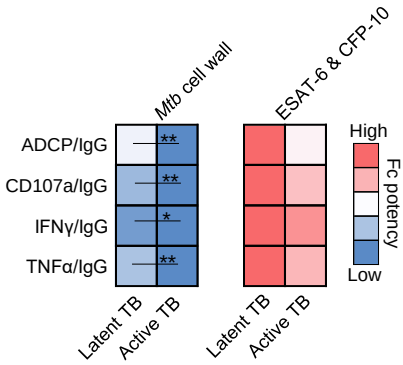

Supplemental Figure 6. *Mtb* cell wall, not ESAT-6 & CFP-10, IgG Fc potency is reduced in active compared to latent TB. Heatmap depicts ADCP and markers of ADNKA normalized by antigen specific IgG titers to determine functional potency. Statistical significance was determined by linear regression to adjust for sex and age. *$P \leq 0.05$ and **$P \leq 0.01$.

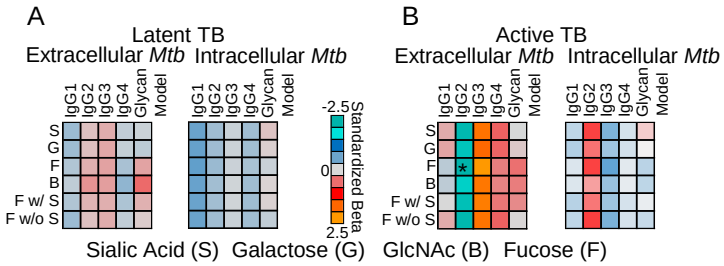

Supplemental Figure 7. ESAT-6 & CFP-10 subclasses and glycans have minimal relationships with *Mtb* burden. Heatmaps show that in **(A)** latent TB and **(B)** active TB, ESAT6 & CFP10 subclasses combined with glycans have limited relationships to intracellular and extracellular *Mtb* burden as determined by multiple linear regression. *$P \leq 0.05$.

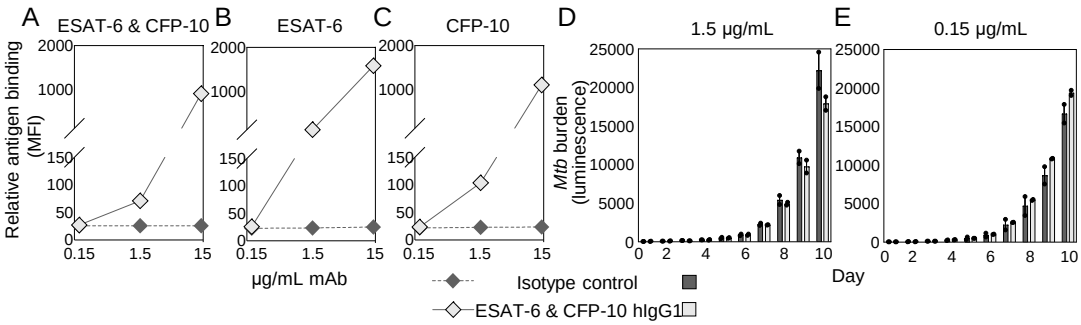

Supplemental Figure 8. A human IgG1 mAb binds ESAT-6 & CFP-10 and does not inhibit intracellular *Mtb* at low doses. Luminex demonstrates relative binding of mAb to ESAT-6 and isotype control CR3022 anti-SARS-CoV-2 RBD hIgG1 to (A) ESAT-6 & CFP-10, (B) ESAT-6, and (C) CFP-10. Treatment of *Mtb* infected macrophages at the low doses of **(D)** 1.5 or **(E)** 0.15µg/mL mAb had limited impact on intracellular burden during macrophage infection. Mean and SEM are shown. There were no significance differences as determined by unpaired t-test.